PMTurkeyCOLPEm Resource

From: Comar, Manny
Sent: Thursday, November 01, 2012 5:05 PM
To: TurkeyCOL Resource
Subject: FW: DRAFT RAI Responses FPL Turkey Point 6 & 7 for eRAI 6024 Basic Geologic and Seismic Information
Attachments: Draft Revised Response for NRC RAI Letter No. 041, RAI 02.05.01-7 (eRAI 6024).pdf; Draft Revised Response for NRC RAI Letter No. 041, RAI 02.05.01-29 (eRAI 6024).pdf; Draft Revised Response for NRC RAI Letter No. 041, RAI 02.05.01-4 (eRAI 6024).pdf; Draft Revised Response for NRC RAI Letter No. 041, RAI 02.05.01-6 (eRAI 6024).pdf

---

From: Franzone, Steve [mailto:Steve.Franzone@fpl.com]
Sent: Saturday, September 29, 2012 9:08 AM
To: Comar, Manny
Cc: Burski, Raymond; Maher, William; Franzone, Steve
Subject: DRAFT RAI Responses FPL Turkey Point 6 & 7 for eRAI 6024 Basic Geologic and Seismic Information

Manny,

To support a future public meeting, FPL is providing draft revised responses for eRAI 6024 (RAI questions 02.05.01-4, 02.05.01-6, 02.05.01-7, 02.05.01-29) in the attached files.

If you have any questions, please contact me.
Thanks

Steve Franzone
NNP Licensing Manager - COLA
"Three Rules of Work: Out of clutter find simplicity; From discord find harmony; In the middle of difficulty lies opportunity." Albert Einstein
561.694.3209 (office)
754.204.5996 (cell)

Hearing Identifier: TurkeyPoint_COL_Public
Email Number: 695

Mail Envelope Properties (377CB97DD54F0F4FAAC7E9FD88BCA6D0B1656EF95A)

Subject: FW: DRAFT RAI Responses FPL Turkey Point 6 & 7 for eRAI 6024 Basic Geologic and Seismic Information
Sent Date: 11/1/2012 5:04:56 PM
Received Date: 11/1/2012 5:05:01 PM
From: Comar, Manny

Created By: Manny.Comar@nrc.gov

Recipients:
"TurkeyCOL Resource" <TurkeyCOL.Resource@nrc.gov>
Tracking Status: None

Post Office: HQCLSTR01.nrc.gov

Files	**Size**	**Date & Time**
MESSAGE	1439	11/1/2012 5:05:01 PM
Draft Revised Response for NRC RAI Letter No. 041, RAI 02.05.01-7 (eRAI 6024).pdf	660453	
Draft Revised Response for NRC RAI Letter No. 041, RAI 02.05.01-29 (eRAI 6024).pdf	609101	
Draft Revised Response for NRC RAI Letter No. 041, RAI 02.05.01-4 (eRAI 6024).pdf	2200976	
Draft Revised Response for NRC RAI Letter No. 041, RAI 02.05.01-6 (eRAI 6024).pdf	279991	

Options
Priority: Standard
Return Notification: No
Reply Requested: No
Sensitivity: Normal
Expiration Date:
Recipients Received:

NRC RAI Letter No. PTN-RAI-LTR-041

SRP Section: 02.05.01 - Basic Geologic and Seismic Information

QUESTIONS from Geosciences and Geotechnical Engineering Branch 2 (RGS2)

NRC RAI Number: 02.05.01-7 (eRAI 6024)

FSAR Section 2.5.1.1.1.2.1.1, "Holocene Stratigraphy of the Florida Peninsula" states that hurricanes complicate the preservation of Pleistocene and Holocene deposits on the east and west coasts of the Florida Peninsula by eroding these deposits and depositing them elsewhere. In order for the staff to evaluate the Holocene geologic record at the site and in support of 10 CFR 100.23 please address the following:

a) Within the context of the Holocene sedimentary record at the site discuss the nature and extent of paleostorm deposits.
b) Provide a discussion that compares and contrasts deposits of Hurricane Andrew or other historical hurricanes, and any paleostorm deposits preserved in the Holocene stratigraphy, with potential tsunami deposits at the site.
c) Provide a figure or a map that illustrates these deposits.

FPL RESPONSE:

Part a) of the response addresses the nature of the Holocene section (i.e., muck and silt lenses or layers within the muck), the extent (lateral distance and depth as described by the borings obtained during the subsurface investigation) and the nature of paleostorm deposits (if any) at the Turkey Point Units 6 & 7 site. Part b) of the response compares and contrasts deposits of Hurricane Andrew or other historical hurricanes, and any paleostorm deposits preserved in the Holocene stratigraphy. Lastly, part c) of the response illustrates the locations of the storm deposits.

a) Within the context of the Holocene sedimentary record at the site discuss the nature and extent of paleostorm deposits.

The Holocene section at the Turkey Point Units 6 & 7 site is classified as marl and wetland soils belonging to the saprist (muck) group. The marl and muck are interpreted to have formed in an anaerobic tidal environment. Saprist soils are generally defined as those in which two-thirds or more of the material is decomposed, and less than one-third of plant fibers are identifiable (FSAR 2.5.1 Reference 276). Eighty-eight borings were drilled and sampled (standard penetration test [SPT] samples in soil, continuous coring in rock) as part of the Turkey Point Units 6 & 7 subsurface investigation. The description of the Holocene section (i.e., muck) in the soil borings across the Units 6 & 7 site (FSAR 2.5.1 Reference 708), includes the thickness, color, hardness, and the presence of organics, silt, roots, and shell fragment contents (Table 1). The muck soils were sampled at the site every 2.5 feet using the SPT geotechnical sampling method. The muck soils are classified under the Unified Soil Classification System in accordance with ASTM D2488-06. Modifiers such as trace (< 5 percent), few (5 to 10 percent), little (15 to 25 percent), some (30 to 45 percent) and mostly (50 to 100 percent) were used to provide an estimate of the percentage of gravel, sand and fines (silt or clay size particles), or other materials such as organics (muck) or shells (Table 2). In general, the thickness of the muck ranges from 0 to approximately 15 feet. Muck is observed in the geotechnical borings and the MASW (multi-

channel analysis of surface waves) survey data across the site. The muck appears to be thicker in the areas of the surficial dissolution features, which act as sediment traps (Table 1, FSAR Figures 2.5.4-229 and 230 and the response to RAI 02.05.04-1). Color ranges from black to light gray, dark grayish brown to light brownish gray, and dark olive brown to light olive brown. Mottled coloration is also noted in the muck. The consistency of the muck is very soft-to-soft. Fibrous internal structure occurs within organic soils in eight of the site borings: B-614, B-625, B-626, B-702, B-715, B-725, B-727, and B-729. The organic content of the muck was visually estimated to vary from some (30–45 percent) to mostly (50-100 percent) (Tables 1 and 2, FSAR 2.5.1 Reference 708). The Holocene surficial deposits have been disturbed intermittently since the 1960s by construction activities (FSAR Figure 2.5.1-337).

Although the muck description in FSAR Subsection 2.5.1.1.1.2.1.1 includes silt, only one sample from boring B-601 (DH) contains “mostly silt.” Trace to some sand is noted in three borings: B-617, B-623, and B-723. Neither the sand nor the silt can be correlated across the site as continuous stratigraphic units. However, fine-grained calcareous material, marl, appears to overlie the muck in six borings: B-736, B-738, B-802, B-810, B-812, and B-813. Laboratory tests indicate that this marl-like material is a fat clay to sandy fat clay (rather than a silt as described in the field) that is light/dark gray to light/dark grayish brown, very soft, moist to wet, with some fine grained sand and strong hydrochloric acid reaction (Table 1 and FSAR 2.5.1 Reference 708). This type of marl forms when the ground surface is flooded for several months each year in the summer followed by a number of dry months during the winter (hydroperiod). During the hydroperiod, the microalgae (periphyton) grow on the water surface. The precipitation of the microalgae from the calcium bicarbonate saturated water creates marl (Reference 1).

Examples of storm deposits discussed in the response to part (b) are not observed in samples obtained from the Turkey Point Units 6 & 7 site subsurface investigation borings. At the Turkey Point Units 6 & 7 site, the marl and muck are interpreted to have formed in an anaerobic tidal environment as indicated by the color (i.e., mottled and a wide range of gray to brown coloration), softness, and wetness descriptions (Table 1). The presence of trace amounts of shells and trace amounts of roots at the ground surface is indicative of a calm environment of deposition that enables plants and organisms to grow and thrive or is indicative of a tidal environment that experienced drought conditions (southeastern Florida experienced a drought from 2006 to 2009, Reference 2). Lastly, the presence of silt in only 1 of the 88 borings and sand in 9 of the 88 borings drilled at the Turkey Point Units 6 & 7 site is not conclusive evidence of either a paleostorm or a paleotsunami deposit at the site.

In summary, the Holocene muck, as described on the Turkey Point Units 6 & 7 boring logs, shows uniform conditions across the site (FSAR Figures 2.5.1-231 and 2.5.1-232). The boring logs contain no sedimentary or sedimentological indicators of paleotsunami or paleostorm deposits such as:

- Erosional channels that are filled with poorly sorted, angular, or subangular siliciclastics containing exotic fragments or coral rubble.
- Continuous layered carbonate fine sand, mud and organic detritus.
- Light layers (i.e., carbonate sand).

- Bioturbated carbonate mud with large amounts of roots and shell fragments.
- Weed or shell overwash deposits (shell hash) (FSAR Figure 2.5.1-348, FSAR 2.5.1 Reference 708 and, Reference 3).

b) Provide a discussion that compares and contrasts deposits of Hurricane Andrew or other historical hurricanes, and any paleostorm deposits preserved in the Holocene stratigraphy, with potential tsunami deposits at the site.

Although preserved storm deposits have not been observed at the Turkey Point Units 6 & 7 site, storm deposits have been observed elsewhere in southern Florida. Storm deposits have been preserved at scattered locations on the east coast of Florida at Biscayne Bay and Soldier Key to Elliot Key. Similar deposits are documented on the west coast at Northwest Cape and Cape Sable in the Gulf Coastal Highlands of the Reticulated Coastal Swamps Physiographic Subprovince. This physiographic subprovince is shown on FSAR Figure 2.5.1-217 and the locations of preserved storm deposits are shown on Figure 1.

The Reticulated Coastal Swamps Physiographic Subprovince has been modified by numerous hurricanes in the past. Hurricanes have modified the environment in this physiographic subprovince as follows:

- Decimation of mangrove forests.
- Removal of sufficient beach sand near the Middle Cape Canal.
- Erosion (steps) in the west-and south-facing coastlines of Cape Sable.
- Alteration of the interior marshes.
- Decimation of marginal wetlands and uplands.
- Intrusion of saltwater into an isolated fresh to brackish lake (Lake Ingraham) within the coastal system (Reference 3).

An example of a historical storm deposit is illustrated in a split core taken from a flood tidal delta in the northwest part of Lake Ingraham (Figure 1) (Figure 79, core 24 of Reference 3). The layered delta sequence has accumulated over the past 70 years (as of 2004), following the opening of the Middle Cape Canal by the 1935 Labor Day Hurricane. From a depth of 0 to 70 centimeters, the split core material, a post-1935 flood tidal delta sequence, is composed of layered carbonate fine sand, mud, and organic detritus. The dark organic detritus is fibrous and likely derived from the tidal input during winter storms from eroding mangrove substrates from the north. The light layers are carbonate sands washed in by tropical storm and hurricane events. The darker layers are organic rich carbonate fine sand and mud swept into Lake Ingraham by prevailing tides and winter storms. From a depth of 70 to 100 centimeters, the underlying split core material is composed of bioturbated light grey-tan carbonate mud with black roots and minor shell fragments (Reference 3).

An example of recent sediments deposited by Hurricane Charley (2004) is located between East Cape and Middle Cape (Figure 1) (Reference 3, Figure 117). The top photograph from Figure 117 of Reference 3 illustrates large weed and shell overwash deposits. The two lower photographs from Figure 117 of Reference 3 illustrate a sharp beach escarpment with a 15-centimeter thick coarse shell layer on top (Reference 3).

During the 20th century, several powerful hurricanes (intensity greater than Category 3 on the Saffir-Simpson Scale) affected Miami-Dade county: Key West Hurricane (1919), The Hurricane of 1926/Fort Lauderdale and Miami Areas (1926), Palm Beach Hurricane (1928), Labor Day Hurricane (1935), Hurricane Donna (1960), Hurricane Cleo (1964), Hurricane Betsy (1965), Hurricane Andrew (1992), Hurricane Opal (1995), and Hurricane Charley (2004). Due to the resulting destruction and loss of life, Hurricane Andrew is well documented in the scientific literature. Swiadek (Reference 4) discusses the damages from Hurricane Andrew to coastal mangroves in Southern Florida. High wind velocities and storm surges are associated with Hurricane Andrew. The high winds and storm surges caused shoreline erosion, which in turn affected the mangroves. Three factors minimized the impacts of the storm surge: 1) the keys in Biscayne National Park acted as an offshore breakwater, 2) the Bahamas Islands and offshore carbonate shoals limited the fetch of hurricane-force winds, and 3) the continental shelf in southeastern Florida is very narrow (Reference 4).

From late August through mid-September 1992, Swiadek (Reference 4) evaluated sedimentary sequences deposited by Hurricane Andrew in southern Florida. These deposits appear to have originated from shoreline erosion elsewhere in southern Florida. On the west coast of Florida, a widespread layer of mud and muddy sand, up to 50 centimeters thick, was deposited in subtidal banks. Also on the west coast, a grayish mud layer 20 to 50 centimeters thick was deposited underwater in protected off-shore depressions and interior bays. On the east coast, a tan to brownish sedimentary layer, up to 50 centimeters thick, was deposited in the depressions along the western margin of Biscayne Bay. Lastly, on the east coast, a grayish mud layer, up to 50 centimeters thick, was deposited on the east side of Biscayne Bay (Figure 1) (Reference 4).

An example of a sequence of sand overwash deposits is illustrated in Figure 27 in Reference 3. It depicts beach (sand) overwash stratigraphy on a beach north of Northwest Cape (Figure 1) (Figures 28A and 28 in Reference 3). The lower sand in the scarp is a washover deposit from the Labor Day Hurricane (1935), overlain by soil, deposited by a Hurricane Donna (1960) washover layer, in turn overlain by soil and capped by a Hurricane Andrew (1992) sand layer.

According to Swiadek (Reference 4), the waters receding from mangrove swamps on the west coast formed ebb deltas along tidal channels and on Cape Sable. On the east coast, from Soldier Key to Elliot Key, vegetation was removed; however, the limestone surface was not affected (Figure 1) (Reference 4).

Generally, the physical attributes of sedimentary deposits that appear to reflect a modern or paleostorm origin are:

- A moderately thick (average > 30 centimeters) sand bed composed of numerous subhorizontal planar lamination organized into multiple lamina sets.
- Maximum bed thickness is near the shore.
- Landward thinning of the deposit is usually abrupt.
- Abundant shell fragments organized in laminations.

- Storm deposit fill in topographic lows with an upper surface along the shore that is relatively uniform in elevation (FSAR 2.5.1 Reference 890).

As discussed in FSAR 2.5.1.1.5, Tsunami Geologic Hazard Assessment:

> Tuttle et al. (FSAR 2.5.1 Reference 889) distinguish tsunami from storm surge deposits, based on a comparison of deposits from the 1929 Grand Banks tsunami and the 1991 Halloween storm. As noted by Tuttle et al. (FSAR 2.5.1 Reference 889), the challenge of discriminating between the two types of deposits was that both tsunami and storm surge processes result in the onshore transport and re-deposition of sediments. Tuttle et al. (FSAR 2.5.1 Reference 889) conclude that four discriminators (included verbatim below) could be used to distinguish between tsunami and storm deposits:
>
> - Tsunami deposits exhibit sedimentary characteristics consistent with landward transport and deposition of sediment by only a few energetic surges, under turbulent and/or laminar flow conditions, over a period of minutes to hours; whereas characteristics of storm deposits are consistent with landward transport and deposition of sediment by many more, less energetic surges, under primarily laminar flow conditions, during a period of hours to days.
> - Both tsunami and storm deposits contain mixtures of diatoms indicative of an offshore or bay ward source, but tsunami deposits are more likely to contain broken valves and benthic marine diatoms.
> - Biostratigraphic assemblages of sections in which tsunami deposits occur are likely to indicate abrupt and long-lasting changes to the ecosystem coincident with tsunami inundations.
> - Tsunami deposits occur in landscape positions, including landward of tidal ponds, that are not expected for storm deposits.
>
> Similarly, Morton et al. (FSAR 2.5.1 Reference 890) characterize the distinction between tsunami and storm deposits as being related to differences in the hydrodynamics and sediment-sorting processes during transport. Tsunami deposition results from a few high-velocity, long-period waves that entrain sediment from the shoreface, beach, and landward erosion zone. Tsunamis can have flow depths greater than 10 meters (33 feet), transport sediment primarily in suspension, and distribute the load over a broad region where sediment falls out of suspension when flow decelerates. In contrast, storm inundation generally is gradual and prolonged, consisting of many waves that erode beaches and dunes with no significant overland return flow until after the main flooding. Storm flow depths are commonly < 3 meters (9.8 feet), sediment is transported primarily as bed load by traction, and the load is deposited within a zone relatively close to the beach (FSAR 2.5.1 Reference 890). A schematic of typical tsunami and storm deposits is shown in FSAR Figure 2.5.1-348. As noted by Dawson and Stewart (FSAR 2.5.1 Reference 891), hurricane deposits are quite different from tsunami deposits. For example, Scoffin and Hendry (FSAR 2.5.1 Reference 892) use coral rubble stratigraphy on Jamaican reefs to identify past hurricane activity, while Perry (FSAR 2.5.1 Reference

> 893) use storm-induced coral rubble in reef facies from Barbados to identify episodes of past hurricane activity.

However, based on Shanmugam's (Reference 5) review, the problem of differentiating paleotsunami from paleostorm deposits is not straightforward. The sedimentary records of both types of deposits can exhibit the following sedimentary features: basal erosional surfaces, anomalously coarse sand layers, exotic boulders, imbricated boulders and gravel clusters with imbrications, chaotic bedding, rip-up mud clasts, normal grading, inverse grading, multiple upward-fining units, landward-fining trend, horizontal planar laminae, cross-stratification, richness of marine fossils, changes in chemical elements, and lastly, sand injection and soft-sediment deformation. There are no reliable sedimentological criteria for distinguishing paleotsunami and paleostorm deposits in various environments. Both paleotsunamis (tsunamis) and paleostorms (storms) can generate identical depositional processes and related sedimentary features (Reference 5).

The Holocene deposits at the Turkey Point Units 6 & 7 site do not contain any of the above indicators of either paleostorm or paleotsunami deposits. There are no moderately thick sand beds, and there is no indication of abrupt thinning of sand deposits landwards. In addition, there are no abundant shell fragments deposited in laminations.

c) Provide a figure or a map that illustrates these deposits.

Since there are no paleostorm or paleotsunami deposits preserved or observed in the borings at the Turkey Point Units 6 & 7 site, there are no data from which a map can be generated. FSAR Figure 2.5.1-337, Surficial Deposits Map, shows the soils to be disturbed at the footprint of the proposed Turkey Point Units 6 & 7 and the existing cooling canals. As discussed in the response to part (b), storm deposits are only intermittently preserved in southern Florida. Storm deposits are preserved at scattered locations in southwest Florida (Reference 3) and on the shorelines of Biscayne Bay (Reference 4). The examples of storm deposits documented by Wanless and Vlaswinkel (Reference 3) and Swiadek (Reference 4) are discussed in part b) of this response and the locations are shown in Figure 1.

Table 1. Descriptions of Muck at the Turkey Point Units 6 & 7 Site

Boring ID	GS Elevation (ft)	Muck top		Muck bottom		Muck Description	Internal Structure (when described in the log)	Modifiers on Silt and Sand (when described in the log)
		Elevation (ft)	Depth (ft)	Elevation (ft)	Depth (ft)			
B-601 (DH)	-1.4	-1.4	0	-3.9	2.5	MUCK, very dark gray, very soft, wet, mostly silt, some organics, trace shells, weak HCL Rx	-	50 to 100% silt
B-602	-1.4	-1.4	0	-4.5	3.1	MUCK, dark gray, very soft, wet, roots, mostly organic, 2.5 ft firm	-	-
B-603	-1.4	-1.4	0	-4.7	3.3	MUCK, light gray, to black, very soft, wet, mostly organics, trace roots, trace shell fragments	-	-
B-604 (DH)	-1.5	-1.5	0	-4.5	3	MUCK, dark grayish brown, very soft, moist, organics	-	-
B-605	-1.7	-1.7	0	-4.2	2.5	MUCK, very dark gray, very soft, moist, mostly organics	-	-
B-606	-1.4	-1.4	0	-4.4	3	MUCK, light brownish gray, very soft, wet, organic, trace shell fragments, 2.5 ft-black, soft	-	-
B-607	-1.5	-1.5	0	-4	2.5	MUCK, light brownish gray to dark olive brown to black, very soft, wet, organic, trace roots and shell fragments, no HCL Rx	-	-
B-608 (DH)	-1.5	-1.5	0	-6	4.5	MUCK: no recovery, 3.5 ft-very dark brown, very soft, wet, organics	-	-
B-609	-1.5	-1.5	0	-3.5	2	MUCK, very pale brown to very dark gray, very soft, wet, mostly organic, strong HCL Rx	-	-
B-610 (DH)	-1.4	-1.4	0	-4.2	2.8	MUCK, pinkish gray to black, very soft, wet, mostly organic, strong HCL Rx	-	-
B-611	-1.5	-1.5	0	-3.5	2	MUCK, very pale brown, mottled, dark gray, very soft, moist, weak HCL Rx	-	-

Table 1. Descriptions of Muck at the Turkey Point Units 6 & 7 Site (continued)

Boring ID	GS Elevation (ft)	Muck top		Muck bottom		Muck Description	Internal Structure (when described in the log)	Modifiers on Silt and Sand (when described in the log)
		Elevation (ft)	Depth (ft)	Elevation (ft)	Depth (ft)			
B-612	-1.5	-1.5	0	-4.5	3	MUCK, grayish brown, very soft, wet, no HCL Rx	-	-
B-613	-1.4	-1.4	0	-4.8	3.4	MUCK, black, very soft, wet, strong, HCL Rx, mostly organics	-	-
B-614	-1.5	-1.5	0	-5.3	3.8	MUCK, black, very soft, wet, **fibrous**, strong HCL Rx, 2.8 ft-soft	fibrous	-
B-615	-1.5	-1.5	0	-6	4.5	MUCK, dark brown, very soft, wet, strong HCL Rx	-	-
B-616	-1.2	-1.2	0	-8.2	7	MUCK, very dark gray, very soft, wet, mostly organics, weak HCL Rx, 2.5 ft-trace shell fragments, weak HCL Rx	-	-
B-616	-1.2	-10.7	9.5	-12.2	11.0	MUCK, brown, firm, wet, with limestone fragments, mostly organics	-	-
B-617	-1.4	-1.4	0	-3.4	2	MUCK, pale brown, very soft, wet, **few fine grained sand**, mostly organic, strong HCL Rx	-	5 to 10% fine grained sand
B-618	-1.4	-1.4	0	-4.4	3	MUCK, very dark grayish brown, very soft, wet, trace peat	-	-
B-619	-1.7	-1.7	0	-5.2	3.5	MUCK, very dark grayish brown, very soft, wet, mostly organic	-	-
B-620 (DH)	-1.5	-1.5	0	-4.5	3	MUCK, light gray, to grayish brown, very soft, wet, strong, HCL Rx, mostly organics	-	-
B-621	0.2	0.2	0	-5.9	6.1	MUCK, very dark gray, very soft, dry, mostly organic, strong HCL Rx	-	-

Table 1. Descriptions of Muck at the Turkey Point Units 6 & 7 Site (continued)

Boring ID	GS Elevation (ft)	Muck top		Muck bottom		Muck Description	Internal Structure (when described in the log)	Modifiers on Silt and Sand (when described in the log)
		Elevation (ft)	Depth (ft)	Elevation (ft)	Depth (ft)			
B-622	0.2	0.2	0	-5.4	5.6	MUCK, light brownish gray, to very dark gray, very soft, moist, mostly organic, strong HCL Rx	-	-
B-623	-1.3	-1.3	0	-5	3.7	MUCK, light brownish gray to very dark gray, wet, mostly organic, strong HCL Rx	-	-
B-624	-1.4	-1.4	0	-4.4	3	MUCK, light olive brown to very dark grayish brown, very soft, wet, organic, strong HCL Rx	-	-
B-625	-1.4	-1.4	0	-4.2	2.8	MUCK, black, very soft, wet, strong HCL Rx, mostly organic, **fibrous**	fibrous	-
B-626	-1.6	-1.6	0	-5.1	3.5	MUCK, black, very soft, wet, no HCL Rx, **fibrous**	fibrous	-
B-627	-1.3	-1.3	0	-4.2	2.9	MUCK, light brownish gray to very dark brown, very soft, wet, organic, trace shell fragments	-	-
B-628	-1.5	-1.5	0	-5.3	3.8	MUCK, light brownish gray, very soft to soft, wet, strong HCL Rx, mostly organic, shell fragments	-	-
B-629	-1.1	-1.1	0	-4.6	3.5	MUCK, brown, very soft, wet, organics, trace shell fragments, strong HCL reaction, 2.5 ft-black	-	-
B-630	-1.5	-1.5	0	-4.5	3	MUCK; no recovery	-	-
B-631	-1.2	-1.2	0	-4.8	3.6	MUCK, very dark gray, wet, very soft, mostly organic, strong HCL Rx	-	-
B-632	-1.6	-1.6	0	-5.1	3.5	MUCK, very dark grayish brown, very soft, wet, strong HCL Rx	-	-

Table 1. Descriptions of Muck at the Turkey Point Units 6 & 7 Site (continued)

Boring ID	GS Elevation (ft)	Muck top		Muck bottom		Muck Description	Internal Structure (when described in the log)	Modifiers on Silt and Sand (when described in the log)
		Elevation (ft)	Depth (ft)	Elevation (ft)	Depth (ft)			
B-633	-1.5	-1.5	0	-4.5	3	MUCK, very dark grayish brown, very soft, wet, strong HCL Rx, organics, trace shell fragments	-	-
B-634	-0.7	-0.7	0	-5.2	4.5	MUCK, very dark gray, very soft, wet, **trace fine grained sand**, trace shell fragments, strong HCL Rx, 2.5 ft-soft, weak HCL Rx	-	<5% fine grained sand
B-635	-0.9	-0.9	0	-2.9	2	Sandy FAT CLAY, very dark gray to very pale brown, very soft, wet, some fine grained sand, trace organics, strong HCL Rx	-	-
B-635	-0.9	-2.9	2	-4.1	3.2	MUCK, very dark gray, very soft, wet, trace shell fragments, mostly organic, weak HCL Rx	-	-
B-636	-1.1	-1.1	0	-4.8	3.7	MUCK, black to gray, very soft, moist, mostly organic, strong HCL Rx	-	-
B-637	-0.2	-0.2	0	-4.2	4	MUCK, very dark grayish brown, very soft, moist, strong HCL Rx	-	-
B-639	-1.4	-1.4	0	-4.4	3	MUCK, black, very soft, wet, organic, trace shells	-	-
B-701 (DH)	-1.1	-1.1	0	-4	2.9	MUCK, olive gray to black, very soft, wet, mostly organic, strong HCL Rx	-	-
B-702	-1.2	-1.2	0	-4.6	3.4	MUCK, very dark grayish brown, very soft, wet, strong HCL Rx, **fibrous**	fibrous	-

Table 1. Descriptions of Muck at the Turkey Point Units 6 & 7 Site (continued)

Boring ID	GS Elevation (ft)	Muck top		Muck bottom		Muck Description	Internal Structure (when described in the log)	Modifiers on Silt and Sand (when described in the log)
		Elevation (ft)	Depth (ft)	Elevation (ft)	Depth (ft)			
B-703	-1.3	-1.3	0	-4.6	3.3	MUCK, very dark grayish brown, very soft, wet, organics, strong HCL Rx, 2.5 ft-soft	-	-
B-704 (DH)	-1.4	-1.4	0	-4.5	3.1	MUCK, greenish brown, very soft, wet, strong HCL reaction, mostly organics, 2.4 ft-grayish brown to dark grayish brown, soft	-	-
B-705	-1.3	-1.3	0	-4.2	2.9	MUCK, very dark brown, very soft, wet	-	-
B-706	-1.2	-1.2	0	-4.4	3.2	MUCK, brown to very pale brown, very soft, moist, organics, strong HCL Rx	-	-
B-707	-1.8	-1.8	0	-3.8	2	MUCK, light brownish gray to very dark gray, very soft, mostly organic, strong HCL Rx	-	-
B-708 (DH)	-1.4	-1.4	0	-3.9	2.5	MUCK, dark gray brown to black, moist, mostly organic, strong HCL Rx	-	-
B-709	-1.3	-1.3	0	-4.6	3.3	MUCK, very dark brown, very soft, moist, organic	-	-
B-710 (DH) R	-1.3	-1.3	0	-3.8	2.5	MUCK, dark grayish brown, to black, very soft, wet, organics, strong HCL Rx	-	-
B-711	-1.1	-1.1	0	-4.1	3	MUCK, grayish brown to light gray, very soft, wet, strong, HCL Rx, mostly organic, 2.5 ft-dark grayish brown	-	-
B-712	-1.1	-1.1	0	-4.2	3.1	MUCK, very dark grayish brown, very soft, moist, mostly organic, strong HCL Rx	-	-

Table 1. Descriptions of Muck at the Turkey Point Units 6 & 7 Site (continued)

Boring ID	GS Elevation (ft)	Muck top		Muck bottom		Muck Description	Internal Structure (when described in the log)	Modifiers on Silt and Sand (when described in the log)
		Elevation (ft)	Depth (ft)	Elevation (ft)	Depth (ft)			
B-713	-1.1	-1.1	0	-3.6	2.5	MUCK, dark grayish brown to pale brown, very soft, wet, mostly organic	-	-
B-714	-1	-1	0	-4.4	3.4	MUCK, olive brown, very soft, wet, strong HCL Rx, mostly organic	-	-
B-715	-0.9	-0.9	0	-4.4	3.5	MUCK, black, very soft, wet, strong HCL Rx, **fibrous**	fibrous	-
B-716	-1.1	-1.1	0	-4.1	3	MUCK, light brownish gray, very soft, wet, mostly organic, trace shell fragments, strong HCL Rx	-	-
B-717	-1.1	-1.1	0	-4.7	3.6	MUCK, dark grayish brown, very soft, wet, mostly organic	-	-
B-718	-1.2	-1.2	0	-4.3	3.1	MUCK, brown to very dark grayish brown, very soft, wet, organic, strong HCL Rx, trace shells, 2.5 ft-very dark gray to black	-	-
B-719	-1.1	-1.1	0	-4.1	3	MUCK, light brownish gray to very dark gray, very soft, wet, mostly organic, strong HCL Rx	-	-
B-720 (DH)	-0.9	-0.9	0	-3.9	3	MUCK, gray, very soft, moist organics, trace roots, strong HCL Rx	-	-
B-721	-1.5	-1.5	0	-5	3.5	MUCK, very dense, gray, very soft, wet, mostly organic, strong HCL Rx, 2.5 ft-very dark brown to dark yellowish brown	-	-

Table 1. Descriptions of Muck at the Turkey Point Units 6 & 7 Site (continued)

Boring ID	GS Elevation (ft)	Muck top		Muck bottom		Muck Description	Internal Structure (when described in the log)	Modifiers on Silt and Sand (when described in the log)
		Elevation (ft)	Depth (ft)	Elevation (ft)	Depth (ft)			
B-722	-1	-1	0	-3.5	2.5	MUCK, light brownish gray to very dark gray, very soft, dry to wet, mostly organic, strong HCL Rx	-	-
B-723	-1	-1	0	-5	4	MUCK, very dark grayish brown, very soft to soft, wet, **trace fine grained sand**, strong HCL Rx	-	<5% fine grained sand
B-724	-0.7	-0.7	0	-5.3	4.6	MUCK, very dark grayish brown, very soft, wet, strong HCL Rx, mostly organic	-	-
B-725	-1	-1	0	-4.5	3.5	MUCK, dark grayish brown, very soft, wet, strong HCL Rx, mostly organic, **fibrous**	fibrous	-
B-726	-1.4	-1.4	0	-4.7	3.3	MUCK, dark olive brown, very soft, wet, strong HCL Rx	-	-
B-727	-1.3	-1.3	0	-5.3	4	MUCK, black, very soft, wet, strong HCL Rx, **fibrous**	fibrous	-
B-728	-1.4	-1.4	0	-4.5	3.1	MUCK, black, very soft, wet, strong HCL Rx	-	-
B-729	-1.2	-1.2	0	-4.5	3.3	MUCK, very dark gray, very soft, wet, organics, strong HCL Rx, **fibrous**, 2.5 ft-soft	fibrous	-
B-730	-1	-1	0	-5	4	MUCK, light brownish gray to black, very soft, wet, strong HCL Rx, trace shell fragments, mostly organic	-	-
B-731	-1.5	-1.5	0	-4	2.5	MUCK, light gray to very dark gray, very soft, wet, mostly organic, strong HCL Rx	-	-

Table 1. Descriptions of Muck at the Turkey Point Units 6 & 7 Site (continued)

Boring ID	GS Elevation (ft)	Muck top		Muck bottom		Muck Description	Internal Structure (when described in the log)	Modifiers on Silt and Sand (when described in the log)
		Elevation (ft)	Depth (ft)	Elevation (ft)	Depth (ft)			
B-732	-1	-1	0	-4.5	3.5	MUCK, light gray to light brownish gray, very soft, moist to wet, strong HCL Rx, some organics, 2.5 ft-very dark grayish brown	-	-
B-733	-1	-1	0	-3.5	2.5	MUCK, no recovery	-	-
B-734	-0.6	-0.6	0	-2.6	2	Sandy LEAN CLAY, very dark grayish brown, very soft, moist, strong HCL Rx	-	-
B-734	-0.6	-2.6	2	-4.6	4	MUCK, black to grayish brown, very soft, wet, no to strong HCL Rx	-	-
B-735	-0.8	-0.8	0	-4.5	3.7	at 0 ft MUCK, no recovery, 2.4 ft-MUCK black, very soft, wet, organics	-	-
B-736	-0.5	-0.5	0	-2.5	2	FAT CLAY with sand, dark grayish brown, very soft, moist, fine grained sand, strong HCL Rx	-	-
B-736	-0.5	-2.5	2	-4.5	4	MUCK, black, very soft, wet, **few sand**, organics, weak HCL Rx	-	5 to 10% sand
B-737	-0.6	-0.6	0	-5.1	4.5	MUCK, light brownish gray, mottled, very dark gray and black, very soft, wet, **little fine grained sand**, trace shell fragments, strong HCL Rx, 2.5 ft-very dark gray, weak HCL Rx	-	15 to 25% fine grained sand
B-738	0.1	0.1	0	-1.9	2	Sandy FAT CLAY, very dark grayish brown, very soft, moist, fine sand, strong HCL Rx	-	-

Table 1. Descriptions of Muck at the Turkey Point Units 6 & 7 Site (continued)

Boring ID	GS Elevation (ft)	Muck top		Muck bottom		Muck Description	Internal Structure (when described in the log)	Modifiers on Silt and Sand (when described in the log)
		Elevation (ft)	Depth (ft)	Elevation (ft)	Depth (ft)			
B-738	0.1	-1.9	2	-4.4	4.5	MUCK, very dark grayish brown, soft, wet, organics, strong HCL Rx	-	-
B-739	-1.6	-1.6	0	-4.6	3	MUCK, light brownish gray, to dark grayish brown, very soft, wet, strong, HCL Rx, mostly organic	-	-
B-802	-1.5	-1.5	0	-3.5	2	Sandy FAT CLAY, light gray, very soft, wet, **some fine grained sand**, trace organics, strong HCL Rx	-	30 to 45% fine grained sand
B-802	-1.5	-3.5	2	-4.8	3.3	MUCK, dark gray to light gray, very soft, moist, fine grained sand, trace shell fragments, strong HCL Rx	-	-
B-805	-1.6	-1.6	0	-4.1	2.5	MUCK, dark grayish brown, very soft, wet, strong HCL Rx, organics	-	-
B-806	-0.4	-0.4	0	-4.9	4.5	MUCK, very dark gray, very soft, wet, mostly organic, strong HCL Rx	-	-
B-807	-0.7	-0.7	0	-4.2	3.5	MUCK, very dark gray, very soft, wet, mostly organic, strong HCL Rx	-	-
B-808	-1	-1	0	-4.4	3.4	MUCK, light gray to grayish brown, very soft, moist to wet, strong HCL Rx, 2.8 ft-dark gray	-	-
B-809	-1.3	-1.3	0	-4.3	3	MUCK, very dark gray, very soft, moist, mostly organic, strong HCL Rx, trace shell fragments	-	-

Table 1. Descriptions of Muck at the Turkey Point Units 6 & 7 Site (continued)

Boring ID	GS Elevation (ft)	Muck top		Muck bottom		Muck Description	Internal Structure (when described in the log)	Modifiers on Silt and Sand (when described in the log)
		Elevation (ft)	Depth (ft)	Elevation (ft)	Depth (ft)			
B-810	-1.2	-1.2	0	-3.2	2	FAT CLAY with sand, light brownish gray, very soft, wet, **some fine grained sand**, trace organics, strong HCL Rx	-	30 to 45% fine grained sand
B-810	-1.2	-3.2	2	-4.3	3.1	MUCK, dark gray, soft, moist, mostly organic, strong HCL Rx	-	-
B-811	-1.4	-1.4	0	-5.3	3.9	MUCK, black, very soft, wet, strong, HCL Rx	-	-
B-812	-1.4	-1.4	0	-2.9	1.5	Sandy FAT CLAY, very pale brown, very soft, wet, **some fine grained sand,** trace organics, trace shell fragments, strong HCL Rx	-	30 to 45% fine grained sand
B-812	-1.4	-2.9	1.5	-4.1	2.7	MUCK, very dark gray, soft, wet, mostly organic, trace shell fragments, strong HCL Rx	-	-
B-813	-1.3	-1.3	0	-3.3	2	Sandy FAT CLAY, dark gray, to gray, very soft, wet, some sand, trace shell fragments, fine grained sand, trace shells, strong HCL Rx	-	-
B-813	-1.3	-3.3	2	-4.8	3.5	MUCK, very dark gray, very soft, wet, trace shell fragments, mostly organic, weak HCL Rx	-	-
B-814	9	9	0	4.5	4.5	Poorly Graded Sand with gravel (Spoil Material)	-	-
B-814	9	4.5	4.5	-3.2	12.2	Poorly Graded Gravel (Spoil Material)	-	-
B-814	9	-3.2	12.2	-6.1	15.1	MUCK, black, very soft, wet, strong HCL Rx, mostly organic	-	-

Table 2. Modifiers

MODIFIERS	
Approximate Percentage	**Modifiers**
<5%	TRACE
5 to 10%	FEW
15 to 25%	LITTLE
30 to 45%	SOME
50 to 100%	MOSTLY

Source: FSAR 2.5.1 Reference 708

Figure 1. Locations of Storm Deposits in Southern Florida

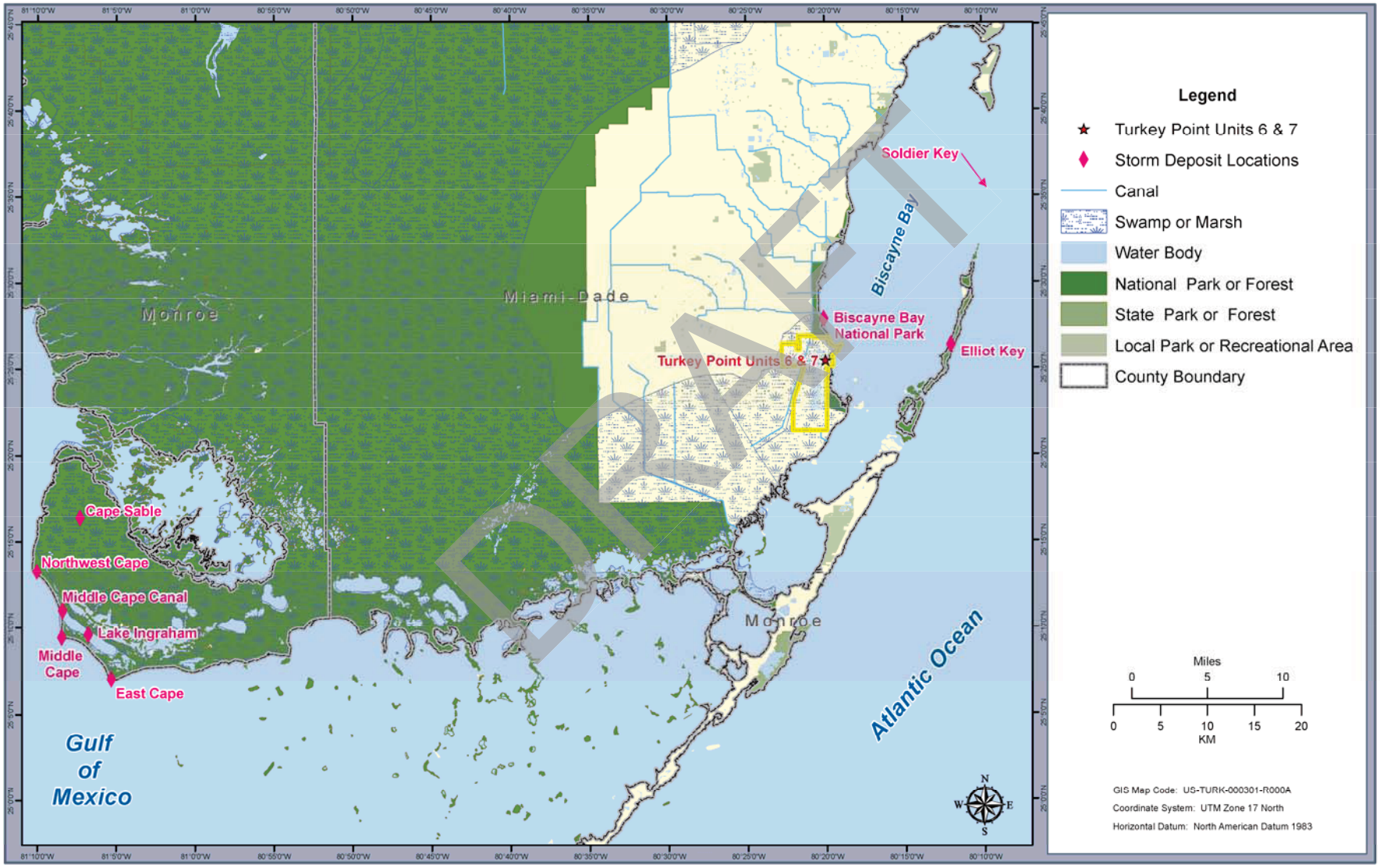
Legend
Turkey Point Units 6 & 7
Storm Deposit Locations
Canal
Swamp or Marsh
Water Body
National Park or Forest
State Park or Forest
Local Park or Recreational Area
County Boundary
Soldier Key
Biscayne Bay
Biscayne Bay National Park
Elliot Key
Turkey Point Units 6 & 7
Miami-Dade
Monroe
Monroe
Cape Sable
Northwest Cape
Middle Cape Canal
Lake Ingraham
Middle Cape
East Cape
Gulf of Mexico
Atlantic Ocean
Miles
0 5 10
0 5 10 15 20
KM
GIS Map Code: US-TURK-000301-R000A
Coordinate System: UTM Zone 17 North
Horizontal Datum: North American Datum 1983
DRAFT

This response is PLANT SPECIFIC.

References:

1. Li, Y. *Calcareous Soils in Miami-Dade County*, Fact Sheet SL 183, Soil and Water Science Department, Florida Cooperative Extension Service, Institute of Food and Agricultural Sciences, University of Florida, 2001.
2. Abtew, W., Pathak, C., Huebner, R.S., and Ciuca, V., "Hydrology of the South Florida Environment," *2010 South Florida Environmental Report,* Vol. I, Chapter 2, p. 73, 2010. Available at http://www.sfwmd.gov/portal/page/portal/pg_grp_sfwmd_sfer/portlet_sfer/tab2236037/2010%20report/v1/chapters/v1_ch2.pdf, accessed August 21, 2012.
3. Wanless., H. R., and Vlaswinkel., B. M., *Coastal Landscape and Channel Evolution Affecting Critical Habitats at Cape Sable, Everglades National Park, Florida,* Final Report to Everglades National Park Service United States Department of Interior, p. 196, 2005.
4. Swiadek, J. W., "The Impacts of Hurricane Andrew on Mangrove Coasts in Southern Florida: A Review," *Journal of Coastal Research*, Vol. 13, No. 1, pp. 242–245, 1997.
5. Shanmugam, G., "Process-sedimentological challenges in distinguishing paleo-tsunami deposits," *Natural Hazards*, Vol. 63, pp. 5–30, 2011.

ASSOCIATED COLA REVISIONS:

The fifth paragraph in FSAR Subsection 2.5.1.2.2 will be replaced with the following paragraphs in a future revision of the FSAR:

The Holocene section at the Turkey Point Units 6 & 7 site is classified as marl and wetland soils belonging to the saprist (muck) group. The marl and muck are interpreted to have formed in an anaerobic tidal environment. Saprist soils are generally defined as those in which two-thirds or more of the material is decomposed, and less than one-third of plant fibers are identifiable (Reference 276). Eighty-eight borings were drilled and sampled (standard penetration test [SPT] samples in soil, continuous coring in rock) as part of the Turkey Point Units 6 & 7 subsurface investigation. The description of the Holocene section (i.e., muck) in the soil borings across the Units 6 & 7 site (Reference 708), includes the thickness, color, hardness, and the presence of organics, silt, roots, and shell fragment contents. The muck soils were sampled at the site every 2.5 feet using the SPT geotechnical sampling method. The muck soils are classified under the Unified Soil Classification System in accordance with ASTM D2488-06. Modifiers such as trace (< 5 percent), few (5 to 10 percent), little (15 to 25 percent), some (30 to 45 percent) and mostly (50 to 100 percent) were used to provide an estimate of the percentage of gravel, sand and fines (silt or clay size particles), or other materials such as organics (muck) or shells. In general, the thickness of the muck ranges from 0 to approximately 15 feet. Muck is observed in the geotechnical borings and the MASW (multi-channel analysis of surface waves) survey data across the site. The muck appears to be thicker in the areas of the surficial dissolution features, which act as

sediment traps (Figures 2.5.4-229 and 230). Color ranges from black to light gray, dark grayish brown to light brownish gray, and dark olive brown to light olive brown. Mottled coloration is also noted in the muck. The consistency of the muck is very soft-to-soft. Fibrous internal structure occurs within organic soils in eight of the site borings: B-614, B-625, B-626, B-702, B-715, B-725, B-727, and B-729. The organic content of the muck was visually estimated to vary from some (30–45 percent) to mostly (50-100 percent) (Reference 708).

Only one sample from boring B-601 (DH) contains "mostly silt." Trace to some sand is noted in three borings: B-617, B-623, and B-723. Neither the sand nor the silt can be correlated across the site as continuous stratigraphic units. However, fine-grained calcareous material, marl, appears to overlie the muck in six borings: B-736, B-738, B-802, B-810, B-812, and B-813. This marl-like material is described as a fat clay to sandy fat clay (rather than a silt as described in the field) that is light/dark gray to light/dark grayish brown, very soft, moist to wet, with some fine grained sand and strong hydrochloric reaction (Reference 708). This type of marl forms when the ground surface is flooded for several months each year in the summer followed by a number of dry months during the winter (hydroperiod). During the hydroperiod, the microalgae (periphyton) grow on the surface water. The precipitation of the microalgae from the calcium bicarbonate saturated water creates marl (Reference 909).

~~The surface of the site consists of approximately 2 to 6 feet (0.6 to 1.8 meters) of organic soils called muck. The muck comprises recent light gray calcareous silts with varying amounts of organic content. The surface elevations for the top of the organic soil ranged from +0.2 to 1.8 feet (0.06 to 0.55 meters) MSL (Figures 2.5.1-334 and 2.5.1-337).~~

The following reference will be added to FSAR Subsection 2.5.1.3 in a future revision of the FSAR.

909. Li, Y. *Calcareous Soils in Miami-Dade County*, Fact Sheet SL 183, Soil and Water Science Department, Florida Cooperative Extension Service, Institute of Food and Agricultural Sciences, University of Florida, 2001.

ASSOCIATED ENCLOSURES:

None

NRC RAI Letter No. PTN-RAI-LTR-041

SRP Section: 02.05.01 - Basic Geologic and Seismic Information

QUESTIONS from Geosciences and Geotechnical Engineering Branch 2 (RGS2)

NRC RAI Number: 02.05.01-29 (eRAI 6024)

FSAR Figure 2.5.1-251, "Lithostratigraphic Map of Cuba", depicts the Matanzas fault zone within the site region; however, the staff notes that the Matanzas fault zone is not discussed in the FSAR.

In order for the staff to assess the tectonic and structural features within the site region and in accordance with 10 CFR 100.23, please address the following questions:

a) Provide a discussion of the Matanzas fault zone in the FSAR, including a larger-scale map showing the fault trace.
b) Clarify if there is a relationship between the Matanzas fault zone and elevated Pleistocene terraces along the coast near Matanzas.
c) Discuss the relationship of the Matanzas fault zone to nearby seismicity.

FPL RESPONSE:

a) Provide a discussion of the Matanzas fault zone in the FSAR, including a larger-scale map showing the fault trace

The terms Matanzas fault and Hicacos fault refer to the same geologic feature. Most newer publications use the term Hicacos fault, and the FSAR follows this convention. The Hicacos fault is discussed in FSAR Subsection 2.5.1.1.1.3.2.4 and is shown in FSAR Figure 2.5.1-247. FSAR Figure 2.5.1-251 is a reproduction of Stanek et al.'s (2009) Figure 2 (FSAR Subsection 2.5.1, Reference 769), which labels this fault as Matanzas fault. The text of FSAR Subsection 2.5.1.1.1.3.2.4 and FSAR Figure 2.5.1-251 will be modified to indicate that Matanzas fault and Hicacos fault are two names for the same geologic feature. Figures 1 and 2 provide larger-scale maps of the Hicacos fault trace.

Garcia et al. (2003) (FSAR Subsection 2.5.1, Reference 489) provide minimal discussion of the Hicacos fault. They indicate it is "a deep fault above Paleocene-Quaternary formations, splitting the ophiolites sequence that makes the main Cuban watershed deviate abruptly, causing different types of fluvial networks" (FSAR Subsection 2.5.1, Reference 489, p. 2571). They state that the "earthquakes reported in Matanzas and more recently in the Varadero-Cardenas area are associated with this structure" (FSAR Subsection 2.5.1, Reference 489, p. 2571). However, no additional information regarding these earthquakes is provided.

Cotilla-Rodríguez et al. (2007) (FSAR Subsection 2.5.1, Reference 494) characterize the Hicacos fault as active based on its possible association with seismicity. Cotilla-Rodriguez et al. (2007) (FSAR Subsection 2.5.1, Reference 494) describe the Hicacos fault as a "normal fault, transcurrent to the left" that is "expressed throughout the Peninsula de Hicacos and is internal in the island territory by the eastern edge of Matanzas Bay, delineating very well the Matanzas Block" (FSAR Subsection 2.5.1, Reference 494, p. 516). Further to the west-southwest, they indicate that the Hicacos fault is "weakly represented"

(FSAR Subsection 2.5.1, Reference 494, p. 516) in the geomorphology. Cotilla-Rodríguez et al. (2007) (FSAR Subsection 2.5.1, Reference 494) indicate a lack of instrumental seismicity associated with the Hicacos fault but suggest that eight earthquakes of MSK intensity III–V (approximately MMI III–V) are located in the general vicinity of the Hicacos fault. They indicate two additional earthquakes in 1854 and 1880 occurred somewhere near the Hicacos fault that were "noticeable without specification [of intensity]" (FSAR Subsection 2.5.1, Reference 494, p. 516). The project Phase 2 earthquake catalog, which is declustered and includes earthquakes M_w 3 and larger, indicates very sparse, minor-magnitude seismicity located near the trace of the Hicacos fault (Figure 1). The nearest epicenters from the project Phase 2 earthquake catalog to the Hicacos fault are four co-located M_w 3.1 to 3.7 earthquakes that occurred near the central portion of the fault in 1812, 1852, 1854, and 1970. Another earthquake occurred in 1777 with M_w 3.7, located on strike with, but approximately 7 miles (11 km) southwest of, the mapped fault trace. Cotilla-Rodriguez et al. (2007) (FSAR Subsection 2.5.1, Reference 494) indicate there are no earthquake focal mechanisms associated with this fault.

Case and Holcombe's (1980) (FSAR Subsection 2.5.1, Reference 480) 1:2,500,000 scale map of the Caribbean region shows segments of the Hicacos fault cutting upper Tertiary rocks. Perez-Othon and Yarmoliuk's (1985) (FSAR Subsection 2.5.1, Reference 848) 1:500,000 scale geologic map of Cuba shows an unnamed fault in the vicinity of the Hicacos fault that extends from Matanzas for approximately 50 miles (80 kilometers) to the southwest (upper panel of Figure 2). Because they do not label faults by name, it is not clear whether the Hicacos fault is depicted on Perez-Othon and Yarmoliuk's (1985) (FSAR Subsection 2.5.1, Reference 848) inset map of fault ages in Cuba. However, they indicate a Mesozoic age for an unnamed fault in the vicinity of the northeastern-most portion of the Hicacos fault. Pushcharovskiy et al.'s (1988) (FSAR Subsection 2.5.1, Reference 846) 1:250,000 scale geologic map of Cuba shows an unnamed fault cutting lower Miocene rocks in the vicinity of the central Hicacos fault, but their mapping does not extend this fault as far northeast as the north coast of Cuba. However, the locally northeast-trending shoreline and a narrow peninsula near Matanzas are notably linear and on-trend with the fault, likely influencing where the fault is mapped in other representations. Pushcharovskiy's (1989) (FSAR Subsection 2.5.1, Reference 847) 1:500,000 scale tectonic map of Cuba shows the northeastern extent of the Hicacos fault similar to the depiction shown in Figure 1 that terminates to the southwest at Cuba's southern coast (middle panel of Figure 2).

The Hicacos fault is depicted differently on various maps from the *Nuevo Atlas Nacional de Cuba* (Reference 2). The 1:1,000,000 scale geologic map from this atlas (Reference 2, plate III.1.2-3) shows an unnamed, northeast-striking, approximately 25-mile-long (40-kilometer-long) fault in the in the vicinity of the Hicacos fault (lowest panel of Figure 2). This unnamed fault is mapped within lower to middle Miocene-age deposits (shown as bright yellow in the lowest panel Figure 2) and does not appear to cut Holocene-age deposits (shown by the gray stippled pattern in the lowest panel of Figure 2) near Matanzas at the northeastern end of the fault. The 1:1,000,000 scale geomorphic map from this atlas (Reference 2, plate IV.3.2-3) shows an unnamed fault offshore along the narrow peninsula that may be the Hicacos fault, but this offshore fault does not extend onshore to the southwest. The Hicacos fault is labeled on the lineament map from this atlas (Reference 2, plate III.3.1-11) as an approximately 110-mile-long (175-km-long), northeast-trending

feature that extends from near Cuba's south coast, across Cuba, and along the narrow peninsula near Matanzas on Cuba's north coast. On the lineament map, the northeastern-most 20 miles (35 kilometers) of this feature are shown as a dashed line. The 1:2,000,000 scale neotectonic map from this atlas (Reference 2, plate III.2.4-8) shows an unnamed, northeast-striking fault in the vicinity of the Hicacos fault that extends from Cuba's south coast, across Cuba, along the narrow peninsula near Matanzas, and offshore where it is terminated by an unnamed fault that likely is the Nortecubana fault.

b) Clarify if there is a relationship between the Matanzas fault zone and elevated Pleistocene marine terraces along the coast near Matanzas

Various researchers describe elevated marine terraces west of Matanzas Bay near the Hicacos fault along Cuba's north coast. Continuous and planar geomorphic surfaces like these can be used as Quaternary strain markers with which to assess the presence or absence of tectonic deformation. Ducloz (Reference 1) and Shanzer et al. (Reference 4) provide observations of three Pleistocene-age terraces in this region. The first (youngest) of these is the Terraza de Seboruco terrace, which is currently a few meters above sea level. Shanzer et al. (Reference 4) document heights of between 3 and 5 meters above sea level for this terrace. The second terrace, the Terraza de Yucayo (Reference 1), is found at 8–10 meters above sea level near Havana, and between 15–25 meters above sea level in the northwest portion of Matanzas (Reference 4). The third terrace, the Terraza de Rayonera, is found at 20–25 meters above sea level near Havana and at no less than 23–25 meters above sea level in the northwest portion of Matanzas (Reference 1). Shanzer et al. (Reference 4) note a minimum height of 35–40 meters above sea level for this terrace in Matanzas. Both Ducloz (Reference 1) and Shanzer et al. (Reference 4) speculate that Pleistocene-age terraces in this region may have formed as the result of both tectonic uplift and global fluctuations in sea level. Shanzer et al. (Reference 4) speculate that the lower terrace elevations near Havana could be the result of differential tectonic uplift between Havana and Matanzas, although no causative faults are identified by the authors. Alternatively, these differences in elevation could be the result of erosion or miscorrelation of surfaces (Reference 5).

More recent studies conclude that ongoing tectonic uplift is not required to explain the present elevations of terraces in northern Cuba near the Hicacos fault. Toscano et al.'s (Reference 5) radiometric age dating of coral samples collected from the Terraza de Seboruco terrace indicates this surface formed at approximately 120–140 ka. Based on extensive literature review performed for this project, to FPL's knowledge, the Terraza de Seboruco is the only terrace in northern Cuba for which radiometric age control is available. Based on these ages, Toscano et al. (Reference 5) associate the Terraza de Seboruco terrace with the global Substage 5e sea level high-stand at approximately 122 ka.

Toscano et al. (Reference 5) also observe that this terrace in the Matanzas area is just a few meters above mean sea level, similar to the elevation of other Substage 5e reef deposits throughout "stable" portions of the Caribbean, and therefore can be explained solely by changes in sea level. Toscano et al. (Reference 5) conclude that "no obvious tectonic uplift is indicated for this time frame along the northern margin of Cuba" (Reference 5, p. 137). Similarly, Pedoja et al. (Reference 3) investigated late Quaternary coastlines worldwide and observe minor uplift relative to sea level of approximately 0.2 millimeters per year, even along passive margins, outpacing eustatic sea level decreases by a factor of

four. They suggest that the Substage 5e terrace in the Matanzas area has been uplifted at an average rate that, when accounting for eustatic changes in sea level, ranges from approximately 0.00 to 0.04 millimeters per year over the last approximately 122 ka, consistent with uplift rates observed from other stable margins worldwide. If the effects of eustasy are ignored, Pedoja et al.'s (Reference 3) data allow for an uplift rate at Matanzas of approximately 0.06 millimeters per year over the last approximately 122 ka, following this "conservative" (Reference 3, p. 5) approach.

Whereas recent studies indicate that tectonic uplift is not required to explain the present elevation of the Terraza de Seboruco terrace west of Matanzas Bay (Reference 5 and Reference 3), these data do not preclude activity on the Hicacos fault. As described above, the location and extent of the Hicacos fault differs between various geologic maps and published figures, so it is unclear whether the Hicacos fault is overlain by the Terraza de Seboruco terrace. Furthermore, if the sense of slip on the Hicacos fault were primarily strike-slip as opposed to dip-slip, it could be difficult to observe surface manifestation of fault-related deformation on the Terraza de Seboruco terrace.

c) Discuss the relationship of the Matanzas fault zone to nearby seismicity

As in most of Cuba, the association of seismicity with individual faults in the Matanzas Bay area is problematic due to the uncertainties associated with the locations of both earthquakes and mapped faults. Cotilla-Rodriguez et al. (2007) (FSAR Subsection 2.5.1, Reference 494) indicate that, due to the lack of seismic stations in the area, there are no instrumental records of earthquakes on the Hicacos fault and that there are no earthquake focal mechanisms associated with this fault. Cotilla-Rodriguez et al. (2007) (FSAR Subsection 2.5.1, Reference 494) do, however, suggest that 10 intensity-based epicenters may be associated with the Hicacos fault. They suggest that eight earthquakes of MSK intensity III–V (approximately MMI III–V) are located in the general vicinity of, and may have occurred on, the Hicacos fault in 1812, 1843, 1852, 1854, 1914 (two earthquakes), 1974, and 1978. Additionally, they suggest two other earthquakes with intensity "noticeable without specification" (FSAR Subsection 2.5.1, Reference 494, p. 516) that may also have occurred on the Hicacos fault in 1854 and 1880.

The project Phase 2 earthquake catalog, which is declustered and includes earthquakes M_w 3 and larger, indicates very sparse, minor-magnitude seismicity associated with the trace of the Hicacos fault (Figure 1). The nearest epicenters from the project Phase 2 earthquake catalog to the Hicacos fault are four co-located M_w 3.1 to 3.7 earthquakes that occurred near the central portion of the fault in 1812, 1852, 1854, and 1970. Another earthquake from the project Phase 2 earthquake catalog occurred in 1777 with M_w 3.7, located on strike with, but approximately 7 miles (11 kilometers) southwest of, the mapped fault trace. It is possible that at least some of these minor-magnitude earthquakes occurred on the Hicacos fault. It is also possible that these earthquakes occurred on some other fault or faults in the region. In the absence of well-located hypocenters, focal mechanisms, and surface faulting for these earthquakes, these earthquakes cannot be definitively attributed to a particular fault or faults.

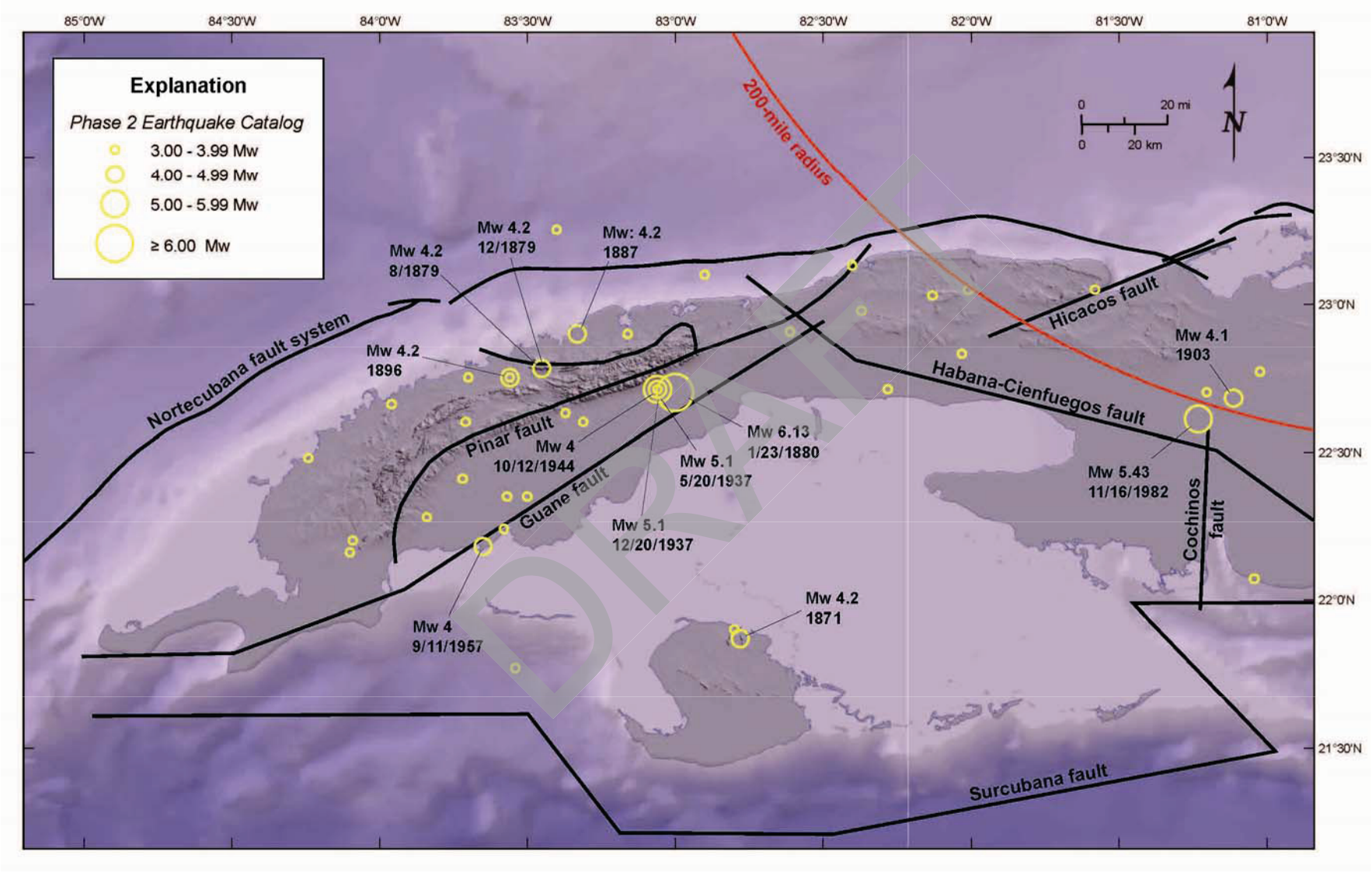

Figure 1. Fault Map of Western Cuba Showing Earthquakes from the Project Phase 2 Earthquake Catalog

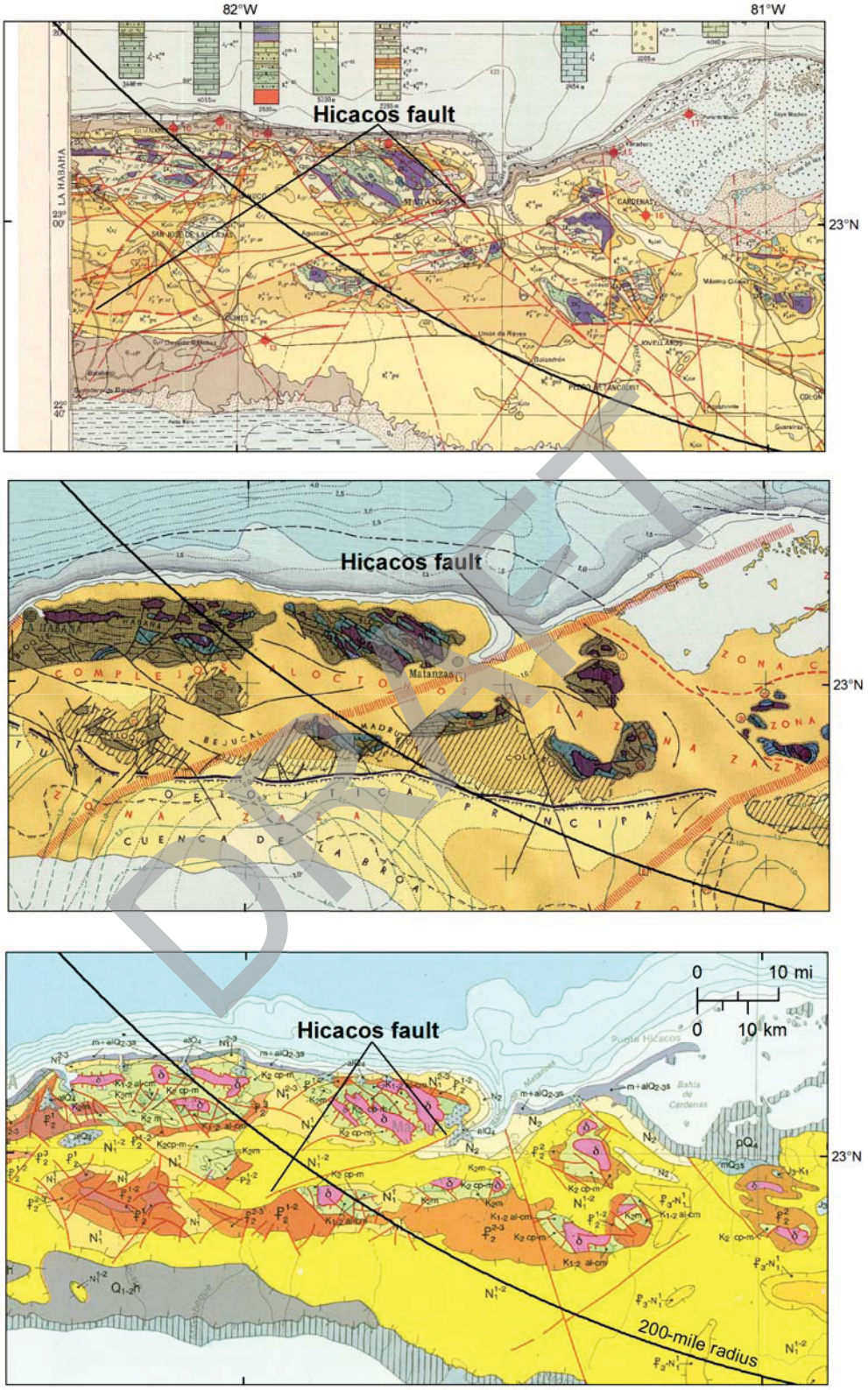

Figure 2. Various mapped depictions of the Hicacos fault. Upper panel modified after Perez-Othon and Yarmoliuk's (1985) (FSAR Subsection 2.5.1, Reference 848) 1:500,000 scale geologic map of Cuba. Middle panel modified after Pushcharovskiy's (1989) (FSAR Subsection 2.5.1, Reference 847) 1:500,000 scale tectonic map of Cuba. Lower panel modified after the 1:1,000,000 scale geologic map from the 1989 *Nuevo Atlas Nacional de Cuba* (Reference 2)

This response is PLANT SPECIFIC.

References:

None

ASSOCIATED COLA REVISIONS:

A discussion of marine terraces will be included in a future update to the FSAR, as detailed in the response to RAI 02.05.01-22.

The discussion of Cuban faults in FSAR Subsection 2.5.1.1.1.3.2.4 will be revised in a future update to the FSAR, as detailed in the response to RAI 02.05.01-21.

The footnote to FSAR Table 2.5.1-204 will be revised in a future update to the FSAR.

c) Mapa Geologico de la Republica de Cuba (Reference 848) ~~(Figure 2.5.1-288)~~

The following note will be added to FSAR Figure 2.5.1-251 in a future update of the FSAR.

Note: The Matanzas fault shown here is the same structure as the Hicacos fault shown on Figure 2.5.1-247.

ASSOCIATED ENCLOSURES:

None

NRC RAI Letter No. PTN-RAI-LTR-041

SRP Section: 02.05.01 - Basic Geologic and Seismic Information

QUESTIONS from Geosciences and Geotechnical Engineering Branch 2 (RGS2)

NRC RAI Number: 02.05.01-4 (eRAI 6024)

FSAR Table 2.5.1-203 "Florida's Marine Terraces, Elevations, and Probable Ages" depict a characterization of nine marine terraces in Florida, however, the staff notes, that the source of this data is 40 years old.

In order for the staff to determine if the information presented in the FSAR represents an up-to-date and accurate characterization of the regional and local geomorphology and in support of 10 CFR 100.23 please address the following:
Incorporate information from more recently-published references (such as those cited in Muhs et al., 2011[a]).

> [a] Muhs, D.R., et al., 2011, Sea-level history of the past two interglacial periods: New evidence from U-series dating of reef corals from south Florida: Quaternary Science Reviews, doi:10.1016/j.quascirev.2010.12.019

FPL RESPONSE:

As discussed in FSAR Subsection 2.5.1.1.1.1.1, Ward et al. (FSAR 2.5.1 Reference 260), Bryan et al. (FSAR 2.5.1 Reference 271), and Healy (FSAR 2.5.1 Reference 261) developed a statewide model and maps of marine terraces in the state of Florida (FSAR Table 2.5.1-203 and FSAR Figure 2.5.1-220). More recent studies have refined the ages of previously mapped marine terraces in Florida, and refined the Pleistocene record of marine terrace development in southern Florida and the Florida keys.

The marine terraces in FSAR Table 2.5.1-203 were once thought to be the direct result of sea level fluctuations through the last glacial cycles, but are now understood to be a result of complex interactions between sea-level oscillation, subaerial exposure, a precipitation-karstification function, and isostatic uplift (FSAR 2.5.1 Reference 262 and Reference 1). Recently, researchers modeled terraces in southeast Florida (Reference 1) and collected corals for radiometric age dating using the $^{234}U/^{238}U$ isotopes to back calculate sea levels associated with those terraces during the Pleistocene (References 2 through 6). Since reefs form in a shallow marine environment, the organisms that comprise the Key Largo and Miami limestones preserve the record of Pleistocene sea level changes. These limestones in some places have been subaerially exposed. Investigators (References 2 through 6) studied the aforementioned limestones to understand the Atlantic-Caribbean sea level changes. The record of Pleistocene sea level changes is preserved in the marine sequences Q1 through Q5, from oldest to youngest, which correlate to marine isotope stages MIS 11, 9, 7, and 5e (Table 1) (Reference 2). The marine sequences are defined as a stratigraphic sequence of marine strata that represents a population of benthic organisms. Marine isotope stages (MIS) are alternating warm and cool periods in the Earth's paleoclimate history, inferred from oxygen isotope data reflecting changes in temperature.

Adams et al. (Reference 1) generated a model that calculates lithospheric uplift as a result of a precipitation-driven karstification function (decrease of bulk crustal density) and variations in subaerial exposure of a carbonate platform (i.e. Florida) due to oscillating sea level. The authors applied this model to north-central Florida to estimate the ages of beach ridges and depositional coastal terraces. The ages were based on the most recent estimates of sea level history since the Pliocene. The modeled ages of sea level highstands were then compared to the elevations of uplifted beach ridges and coastal terraces to evaluate plausible ages for deposition of the observed coastal geomorphic features (Reference 1). The geomorphic features were the Trail Ridge, the Penholoway Terrace, and the Talbot Terrace (Figure 1). The model produced the following ages for the three geomorphic features near the north Florida-southeastern Georgia Atlantic coast: (1) Trail Ridge approximately 1.44 m.y., (2) Penholoway Terrace approximately 408 k.y, and (3) Talbot Terrace approximately 120 k.y. (FSAR Table 2.5.1-203; Reference 1).

Hickey et al. (Reference 2) analyzed the $^{234}U/^{238}U$ ages of cores recovered at Grossman Ridge Rock Reef and Joe Ree Rock Reef in the Florida Everglades and revealed additional subaerial-exposure surfaces that are used to delineate subdivisions within the five marine sequences of the Pleistocene carbonates of south Florida (Figure 2). These five marine sequences with Hickey et al. (Reference 2) subdivisions in parentheses are as follows: Q1 (Q1a-Q1b), Q2 (Q2a-Q2d), and Q4 (Q4a-Q4b) and Q5 (Q5e) (Figure 3). These subdivisions delineated by Hickey et al. (Reference 2) within units Q1 through Q5 preserve evidence of at least ten separate sea-level highstands, rather than five as indicated by previous studies (i.e. Perkins, 1977, and Harrison et al., 1984) (Reference 2). Q5e is the youngest Pleistocene subaerial exposure surface of the Florida Keys (Figure 3). The fossil content and the $^{234}U/^{238}U$ radiometric ages indicate that this morphostratigraphic unit was deposited during the peak sea level of the last interglacial marine isotope substage 5e (MIS 5e). Uranium-series ages on corals from this unit from Windley Key, Upper Matecumbe Key, and Key Largo range from 130 to 121 ka after corrections for calculated high initial $^{234}U/^{238}U$ content (Reference 2). A Q4a sample from Point Pleasant near the island of Key Largo has a best estimate age range of 340-300 ka, which falls into the early part of marine-isotope stage 9 (MIS 9) (Reference 2). The age of a Q4b coral sample recovered from a spoil pile in a quarry within unit Q4 on Long Key, southwest of Key Largo is approximately 235 ka (corrected for calculated high initial $^{234}U/^{238}U$). This is consistent with the early part of MIS 7. Hickey et al. (Reference 2) concludes that the Q1 through Q3 units predate MIS 9 and that their preferred interpretation is that Q3 was deposited during MIS 11 and that Q2 and Q1 represent pre-MIS 11 interglacial intervals (Figure 4) (Reference 2). Lastly, Muhs et al. (Reference 3) obtained ages of corals from Windley Key, the island of Key Largo, and from Long Key to Spanish Harbor Keys (middle Florida Keys) using Uranium-series dating. $^{234}U/^{238}U$ age dates are as follows: approximately 114 to 122 ka (Windley Key), approximately 120 to 123 ka (island of Key Largo), and approximately 114 ka (Long Key to Spanish Harbor Keys) (Reference 3). Thus the ages obtained by Muhs et al (References 3 and 7) correlate to MIS 5e and are consistent with the dates obtained by Hickey et al. (Figures 4 and 8 and Table 1) (Reference 2).

Although, no post-Stage 5e dates have been reported from corals recovered from pits or cores from the exposed Florida Keys, several younger dates have been obtained from submerged corals recovered from the shelf to the east of the Florida Keys (References 4 and 5). These have been assigned to marine-isotope substages 5c, 5b, and 5a. These

post-Q5e interglacial highstands were not high enough to flood the south Florida inner platform (Reference 2). Multer et al. (Reference 4) obtained dates for the Key Largo Limestone using thermal ionization mass-spectrometric (TIMS) U-Th dating. The dates from these rocks, 112.4 to 77.8 ka, correspond to the marine-isotope substages 5c and 5a (MIS 5c and MIS 5a). These rocks were found under the shelf edge at Conch Reef, Looe Key, under Carysfort Light area and at the shelf edge near Molasses Reef (Figures 5, 6, and 7) (Reference 4). Toscano and Lundberg (Reference 6) also used TIMS U-Th dating and obtained dates of 7.7 +/- 0.7 ka and 8.6 +/-0.1 ka (basal Holocene) above the unconformity on the shelf edge (core SKSE) at Sand Key outlier reef (lower Keys) (Figures 5 and 6) (Reference 6). Below the unconformity, Toscano and Lundberg (Reference 5) obtained TIMS U-Th dates on corals from Sand Key outlier reef and Carysfort Light area of 86.2 +/- 1.01 and 80.9 +/-1.7 ka (Figures 7 and 8).

Marine terraces in southern Florida, as documented in the studies described above, provide a framework for understanding the Quaternary geomorphic evolution of the site region. The marine terraces in Florida preserve a record of the complex interactions between sea-level oscillation, subaerial exposure, a precipitation-karstification function, and isostatic uplift (FSAR 2.5.1 Reference 262 and Reference 1).

Table 1. Marine Terrace Sequences in Southern Florida

Epoch	Litho-stratigraphic Unit	Marine Sequence Stratigraphic Unit	Radiometric Age Date (ka)	Sample Location	Depth/Elevation	MIS
Pleistocene	Key Largo Limestone\Miami Limestone	Q5e (youngest)	130-121	Windley Key, Upper Matecumbe Key and Key Largo	~4.9 to 5.3 meters above sea level at Windley Key Quarry, water depths of ~16 and ~ 22 meters	5e
		Q5c Q5a	112.4 to 77.8	Conch Reef, Looe Key, Carysfort Light area and Molasses Reef	water depth of -15.2 and -15.5 meters (Carysfort Light area)	5c 5a
		Q4b?	230-220	Long Key Quarry	~0.7 to 3.5 meters above sea level	7
		Q4a	340-300	Point Pleasant Core	NR	9
	Fort Thompson Formation	Q3 Q2 Q1 (oldest)	*** *** ***	Grossman Ridge Rock Reef and Joe Ree Rock Reef	NR	11 11 11?

Source: References 2, 3, 4, and 7

Notes:
"?" uncertainty
*** no reliable dates (Reference 2)
NR- elevations are not recorded in Reference 2
The Radiometric Age Date column is derived from Uranium-series ages ($^{234}U/^{238}U$) on corals and thermal ionization mass-spectrometric Uranium-Thorium (TIMS U-Th) dating.
The Depth Column is approximate.

Figure 1. Locations of the Trail Ridge, Penholoway Terrace and Talbot Terrace in northern Florida and southern Georgia

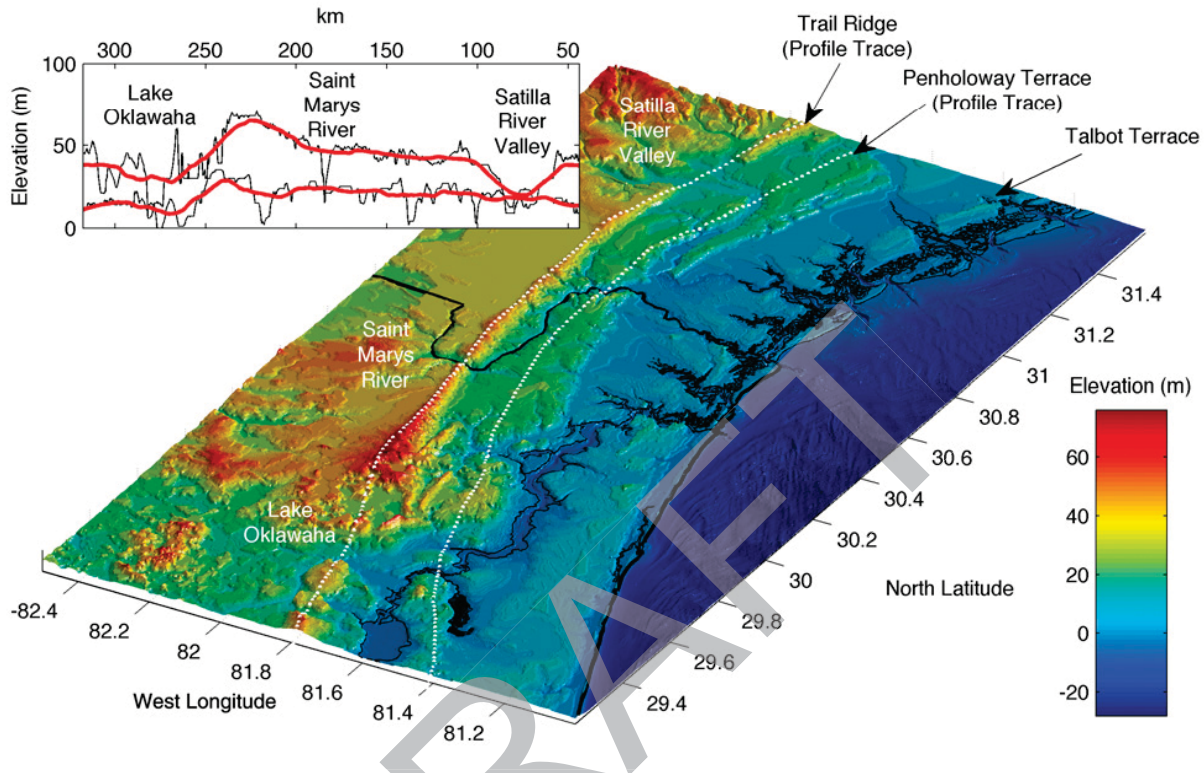

Source: Reference 1

Note: Oblique hillshade image of northern Florida and southern Georgia showing Trail Ridge, modern shoreline, and karstified central Florida. The inset is a profile along Trail Ridge axis showing spatial variation in uplift, which agrees with spatial variation in karstification and/or lithology (Reference 1).

Figure 2. Joe Ree Rock Reef and Grossman Ridge Rock Reef Locations in south Florida in relation to the Turkey Point Units 6 & 7 Site

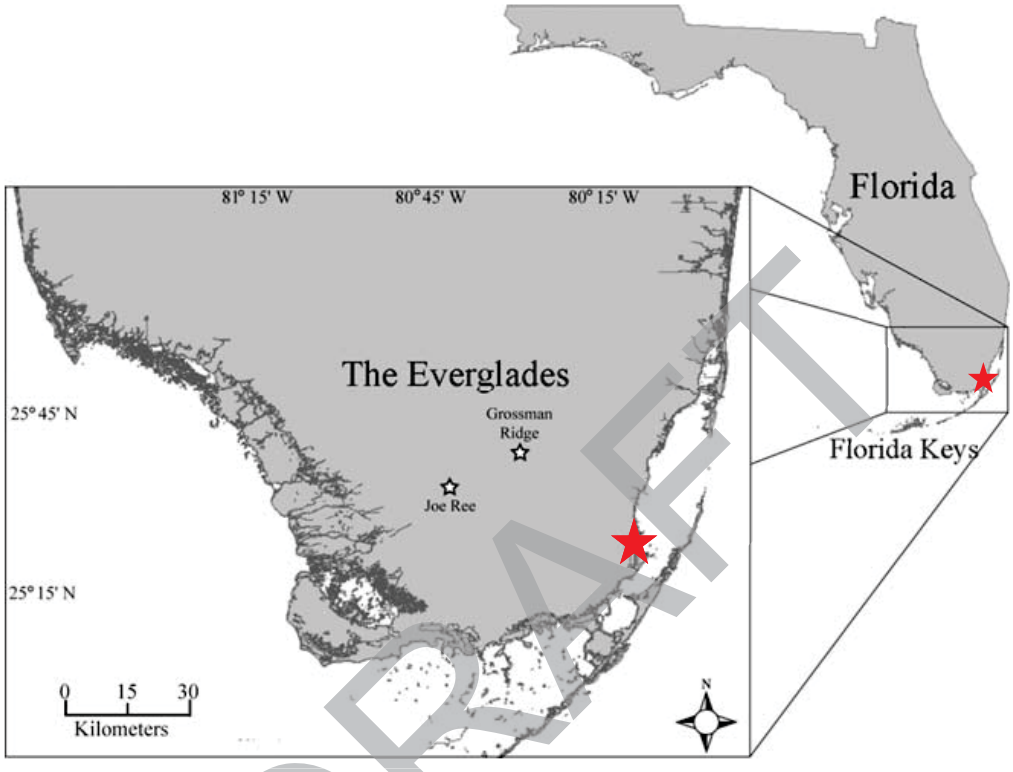

Source: modified from Reference 2

Figure 3. Correlation of marine sequences of the Fort Thompson Formation and Miami Limestone

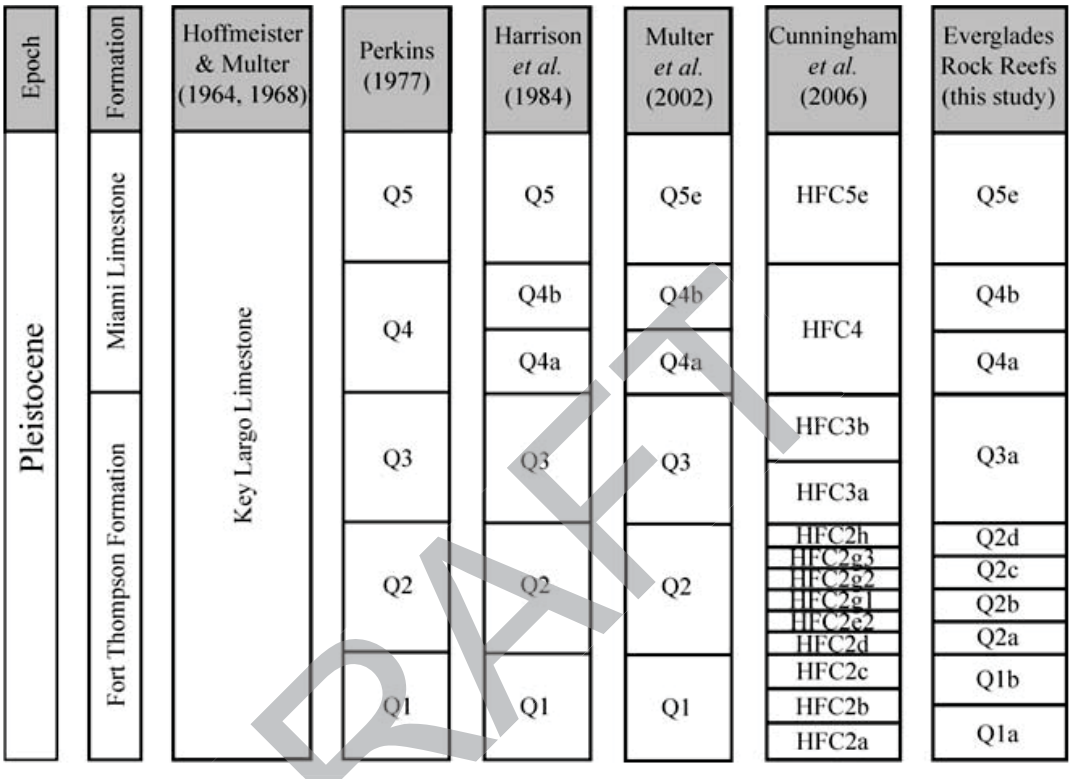

Source: Reference 2

Figure 4. Interpreted correlation of south Florida Pleistocene sea level record

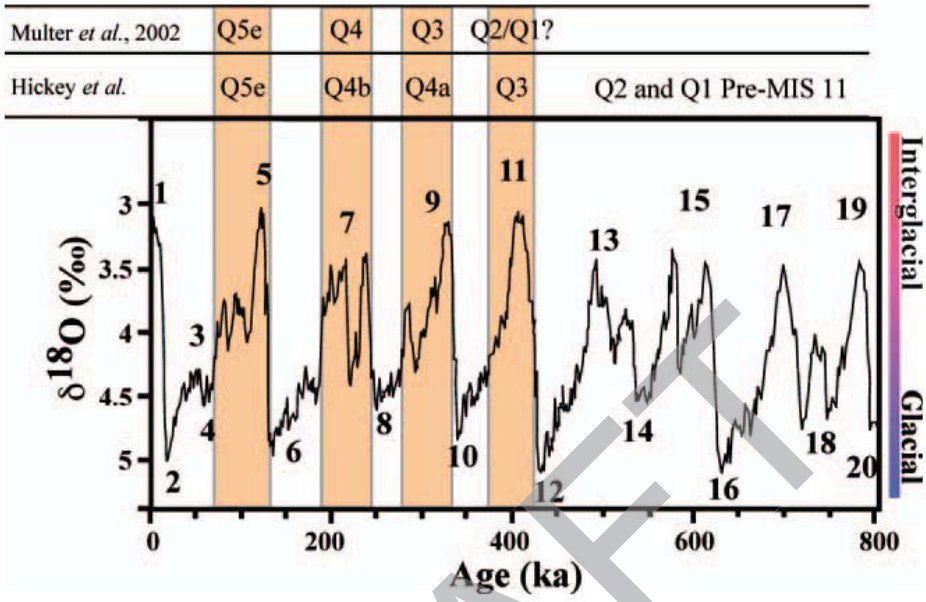

Source: Reference 2

Figure 5. Carysfort Outlier Reef and Sand Key Outlier Reef Locations in south Florida in relation to the Turkey Point Units 6 & 7 Site

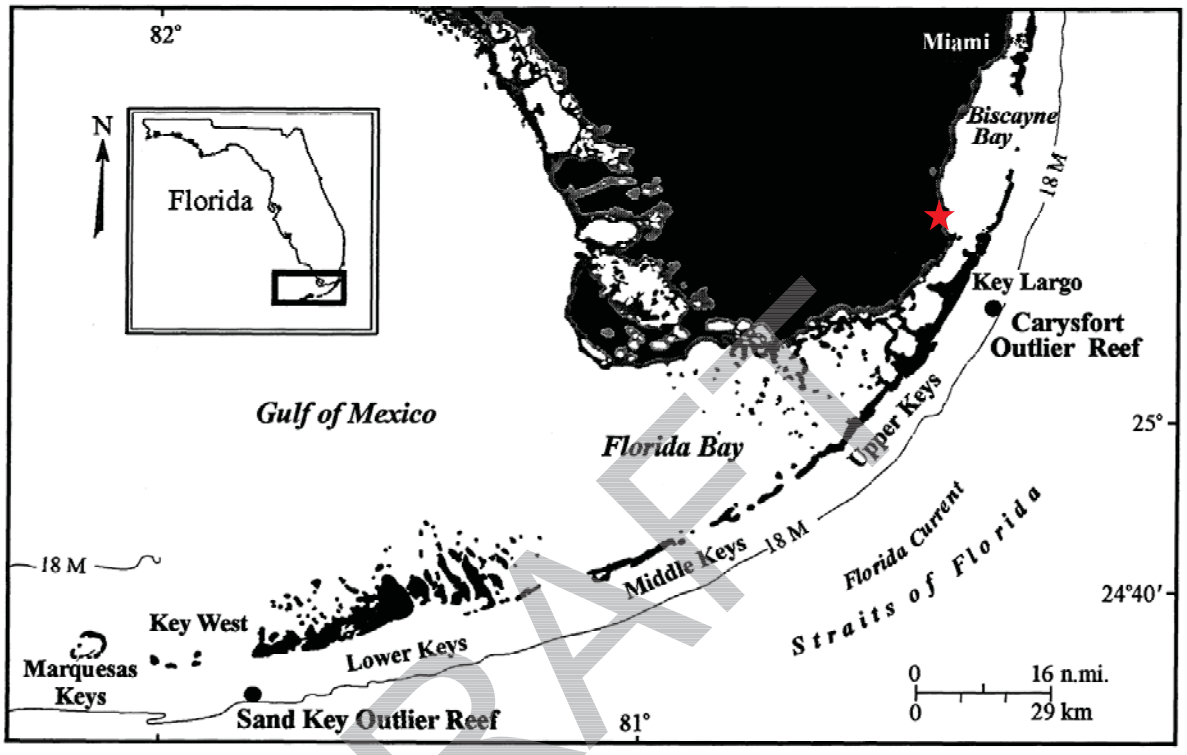

Source: modified from Reference 5

Figure 6. Schematic cross sections of the Sand Key Outlier Reef and the Carysfort Outlier Reef

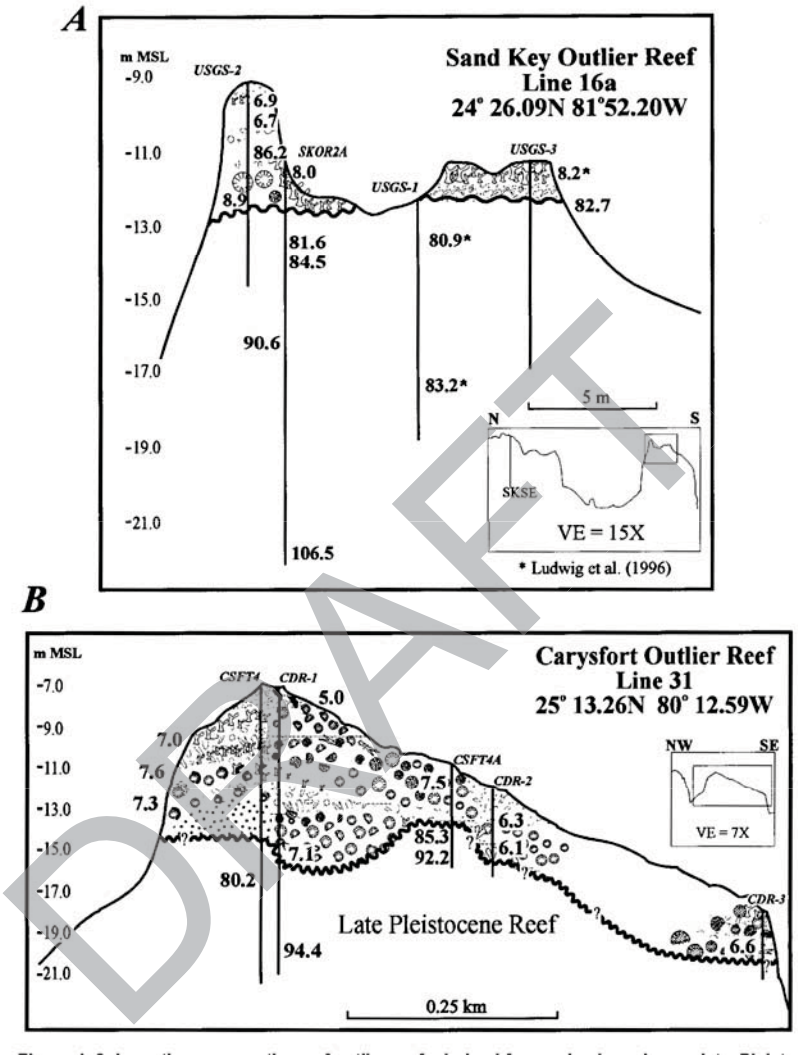

Source: Reference 6

Note: Interpreted cross sections for Sand Key (main outlier reef) and Carysfort Outlier Reef. All dates were determined via the high-precision TIMS U-Th technique. Unconformities were placed using U-Th dates and stable isotope data differentiating marine units from subaerial exposure horizons (Reference 6). All Pleistocene U-Th dates indicate *in situ* post-Substage 5e reef growth. A: Sand Key Cross Section: One Pleistocene date of 86.2 ka in core SKOR2A is considered to be reworked into the associated rubble-pinnacle feature. B: Carysfort Cross Section: All cores are shown. An *A. palmata* reef crest occurs in core CSFT4A (Reference 6).

Figure 7. Composite cross section of the Florida Keys from northwest to southeast and U-series ages of corals from Quaternary reefs.

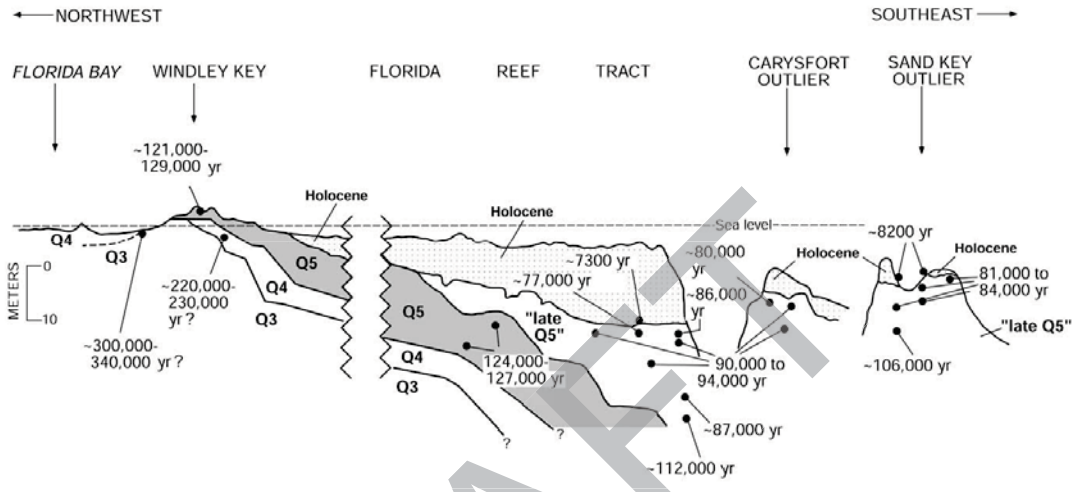

Source: Reference 7

Figure 8.. State of Florida showing modern last glacial and last interglacial shorelines in relation to the Turkey Point Units 6 & 7 Site

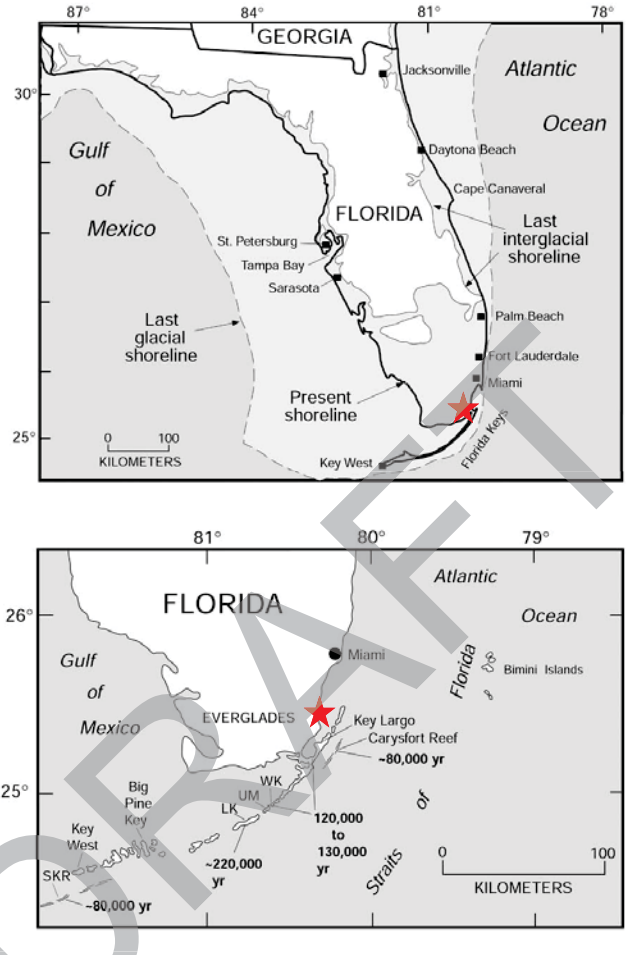

Source: modified from Reference 7

Notes: Upper: Map of the State of Florida, showing the modern, last glacial (~21,000 years), and last interglacial (~120,000 years) shorelines. Lower: detail of southern Florida, including the Florida Keys, and U-series ages of emergent or shallow-submerged Pleistocene reefs. Abbreviations: WK, Windley Key, UM, Upper Matecumbe Key; LK, Long Key; SKR, Sand Key Reef (Reference 7).

This response is PLANT SPECIFIC.

References:

1. Adams, P.N., Opdyke, N.D., Jaeger, J. M., Isostatic uplift driven by karstification and sea-level oscillation: modeling landscape evolution in north Florida. Geology, v. 38, pp. 531-534, 2010.
2. Hickey, T.D., Hine, A.C., Shinn, E.A., Kruse, S.E., Poore, R.Z., Pleistocene carbonate stratigraphy of south Florida: evidence for high-frequency sea-level cyclicity. Journal of Coastal Research, v. 26, pp. 605-614, 2010.
3. Muhs, D.R., Simmons, K.R., Schumann, R.R., and Halley, R. B., "Sea-level history of the past two interglacial periods: new evidence from U-series dating of reef corals from south Florida," Quaternary Science Reviews, v. 30, pp. 570-590, 2011.
4. Multer, H.G., Gischler, E., Lundberg, J, Simmons, K., and Shinn, E.A., Key Largo Limestone revisited: Pleistocene shelf-edge facies, Florida Keys, USA, Facies, v. 46, pp. 229-272, 2002.
5. Toscano, M. A., Lundberg, J., Submerged late Pleistocene reefs on the tectonically-stable S.E. Florida margin: high-precision geochronology, stratigraphy, resolution of substage 5a sea-level elevation, and orbital forcing. Quaternary Science Reviews, v. 18, pp. 752-767, 1999.
6. Toscano, M.A., Lundberg, J., Early Holocene sea-level record from submerged fossil reefs on the southeast Florida margin, Geology, v. 26, pp. 255-258, 1998.
7. Muhs, D. R., Wehmiller, J.F., Simmons, K. R., and York, L., Quaternary sea-level history of the United States, Developments in Quaternary Science, v. 1, pp. 147-183, 2004.

ASSOCIATED COLA REVISIONS:

The following text will be added to Subsection 2.5.1.1.1.1.1.1, sixth paragraph in a future revision of the FSAR as follows:

The marine terraces in Table 2.5.1-203 were once thought to be the direct result of sea level fluctuations through the last glacial cycles, but are now understood to be a result of complex interactions between sea-level oscillation, subaerial exposure, a precipitation-karstification function, and isostatic uplift (Reference 262 and 927). Since reefs form in a shallow marine environment, the organisms that comprise the Key Largo and Miami limestones preserve the record of Pleistocene sea level changes. These limestones in some places have been subaerially exposed. Investigators (References 928 through 933) studied the aforementioned limestones to understand the Atlantic-Caribbean sea level changes. The record of Pleistocene sea level changes is preserved in the marine sequences Q1 through Q5, from oldest to youngest, which correlate to marine isotope stages MIS 11, 9, 7, and 5e (Table 2.5.1-209) (Reference 928). The marine sequences are defined as a stratigraphic sequence of marine strata that represents a population of benthic organisms. Marine isotope stages (MIS) are alternating warm and cool periods in the Earth's paleoclimate history, inferred from oxygen isotope data reflecting changes in temperature.

Adams et al. (Reference 927) generated a model that calculates lithospheric uplift as a result of a precipitation-driven karstification function (decrease of bulk crustal density) and variations in subaerial exposure of a carbonate platform (i.e. Florida) due to oscillating sea level. The authors applied this model to north-central Florida to estimate the ages of beach ridges and depositional coastal terraces. The ages were based on the most recent estimates of sea level history since the Pliocene. The modeled ages of sea level highstands were then compared to the elevations of uplifted beach ridges and coastal terraces to evaluate plausible ages for deposition of the observed coastal geomorphic features (Reference 927). The geomorphic features were the Trail Ridge, the Penholoway Terrace, and the Talbot Terrace (Figure 2.5.1-355). The model produced the following ages for the three geomorphic features near the north Florida-southeastern Georgia Atlantic coast: (1) Trail Ridge approximately 1.44 m.y., (2) Penholoway Terrace approximately 408 k.y, and (3) Talbot Terrace approximately 120 k.y. (Table 2.5.1-203; Reference 927).

Hickey et al. (Reference 928) analyzed the $^{234}U/^{238}U$ ages of cores recovered at Grossman Ridge Rock Reef and Joe Ree Rock Reef in the Florida Everglades and revealed additional subaerial-exposure surfaces that are used to delineate subdivisions within the five marine sequences of the Pleistocene carbonates of south Florida (Figure 2.5.1-356). These five marine sequences with Hickey et al. (Reference 928) subdivisions in parentheses are as follows: Q1 (Q1a-Q1b), Q2 (Q2a-Q2d), and Q4 (Q4a-Q4b) and Q5 (Q5e) (Figure 2.5.1-357). These subdivisions delineated by Hickey et al. (Reference 928) within units Q1 through Q5 preserve evidence of at least ten separate sea-level highstands, rather than five as indicated by previous studies (i.e. Perkins, 1977, and Harrison et al., 1984) (Reference 928). Q5e is the youngest Pleistocene subaerial exposure surface of the Florida Keys (Figure 2.5.1-357). The fossil content and the $^{234}U/^{238}U$ radiometric ages indicate that this morphostratigraphic unit was deposited during the peak sea level of the last interglacial marine isotope substage 5e (MIS 5e). Uranium-series ages on corals from this unit from Windley Key, Upper Matecumbe Key and Key Largo range from 130 to 121 ka after corrections for calculated high initial $^{234}U/^{238}U$ content (Reference 928). A Q4a sample from Point Pleasant near the island of Key Largo has a best estimate age range of 340-300 ka, which falls into the early part of marine-isotope stage 9 (MIS 9) (Reference 928). The age of a Q4b coral sample recovered from a spoil pile in a quarry within unit Q4 on Long Key, southwest of Key Largo is approximately 235 ka (corrected for calculated high initial $^{234}U/^{238}U$). This is consistent with the early part of MIS 7. Hickey et al. (Reference 928) concludes that the Q1 through Q3 units predate MIS 9 and that their preferred interpretation is that Q3 was deposited during MIS 11 and that Q2 and Q1 represent pre-MIS 11 interglacial intervals (Figure 2.5.1-358) (Reference 928). Lastly, Muhs et al. (Reference 929) obtained ages of corals from Windley Key, the island of Key Largo, and from Long Key to Spanish Harbor Keys (middle Florida Keys) using Uranium-series dating. $^{234}U/^{238}U$ age dates are as follows: approximately 114 to 122 ka (Windley Key), approximately 120 to 123 ka (island of Key Largo), and approximately 114 ka (Long Key to Spanish Harbor Keys) (Reference 929). Thus the ages obtained by Muhs et al (References 929 and 933) correlate to MIS 5e and are consistent with

the dates obtained by Hickey et al. (Figures 2.5.1-358 and 2.5.1-362 and Table 2.5.1-209) (Reference 928).

Although, no post-Stage 5e dates have been reported from corals recovered from pits or cores from the exposed Florida Keys, several younger dates have been obtained from submerged corals recovered from the shelf to the east of the Florida Keys (References 930 and 931). These have been assigned to marine-isotope substages 5c, 5b, and 5a. These post-Q5e interglacial highstands were not high enough to flood the south Florida inner platform (Reference 928). Multer et al. (Reference 930) obtained dates for the Key Largo Limestone using thermal ionization mass-spectrometric (TIMS) U-Th dating. The dates from these rocks, 112.4 to 77.8 ka, correspond to the marine-isotope substages 5c and 5a (MIS 5c and MIS 5a). These rocks were found under the shelf edge at Conch Reef, Looe Key, under Carysfort Light area and at the shelf edge near Molasses Reef (Figures 2.5.1-359, 2.5.1-360, and 2.5.1-361) (Reference 930). Toscano and Lundberg (Reference 931) also used TIMS U-Th dating and obtained dates of 7.7 +/- 0.7 ka and 8.6 +/-0.1 ka (basal Holocene) above the unconformity on the shelf edge (core SKSE) at Sand Key outlier reef (lower Keys) (Figures 2.5.1-359 and 2.5.1-360) (Reference 360). Below the unconformity, Toscano and Lundberg (Reference 360) obtained TIMS U-Th dates on corals from Sand Key outlier reef and Carysfort Light area of 86.2 +/- 1.01 and 80.9 +/- 1.7 ka (Figures 2.5.1-361 and 2.5.1-362).

~~The paleoshorelines across the Florida Peninsula are not parallel through time as would be expected by a global rise and drop in sea level.~~ The variations in orientation of shoreline features indicate variations in eustatic adjustment across the Florida Platform and Peninsula (Reference 262). Karstification effectively accomplishes the equivalent of isostatic compensation by decreasing the crustal mass within a vertical column of lithosphere. The rate of karstification (void space creation or equivalent surface lowering rate) within the north Florida Platform is about 3.5 times that of previous estimates (1 meter/11.2 thousand years [k.y.] vs. 1 meter/38 k.y.), and uplift rate is about two times higher than previously thought (0.047 millimeters/year vs. 0.024 millimeters/year) (Reference 262).

The following citation will be added in a future revision of the FSAR as follows:

927. Adams, P.N., Opdyke, N.D., Jaeger, J. M., Isostatic uplift driven by karstification and sea-level oscillation: modeling landscape evolution in north Florida. Geology, v. 38, pp. 531-534, 2010.

928. Hickey, T.D., Hine, A.C., Shinn, E.A., Kruse, S.E., Poore, R.Z., Pleistocene carbonate stratigraphy of south Florida: evidence for high-frequency sea-level cyclicity. Journal of Coastal Research, v. 26, pp. 605-614, 2010.

929. Muhs, D.R., Simmons, K.R., Schumann, R.R., and Halley, R. B., "Sea-level history of the past two interglacial periods: new evidence from U-series dating of reef corals from south Florida," Quaternary Science Reviews, v. 30, pp. 570-590, 2011.

930. Multer, H.G., Gischler, E., Lundberg, J, Simmons, K., and Shinn, E.A., Key Largo Limestone revisited: Pleistocene shelf-edge facies, Florida Keys, USA, Facies, v. 46, pp. 229-272, 2002.

931. Toscano, M. A., Lundberg, J., Submerged late Pleistocene reefs on the tectonically-stable S.E. Florida margin: high-precision geochronology, stratigraphy, resolution of substage 5a sea-level elevation, and orbital forcing. Quaternary Science Reviews, v. 18, pp. 752-767, 1999.

932. Toscano, M.A., Lundberg, J., Early Holocene sea-level record from submerged fossil reefs on the southeast Florida margin, Geology, v. 26, pp. 255-258, 1998.

933. Muhs, D. R., Wehmiller, J.F., Simmons, K. R., and York, L., Quaternary sea-level history of the United States, Developments in Quaternary Science, v. 1, pp. 147-183, 2004.

The following Table and Figures will be added in a future revision of the COLA in the 2.5.1 Subsection.

Table 2.5.1-209. Marine Terrace Sequences in Southern Florida

Epoch	Litho-stratigraphic Unit	Marine Sequence Stratigraphic Unit	Radiometric Age Date (ka)	Sample Location	Depth/Elevation	MIS
Pleistocene	Key Largo Limestone\Miami Limestone	Q5e (youngest)	130-121	Windley Key, Upper Matecumbe Key and Key Largo	~4.9 to 5.3 meters above sea level at Windley Key Quarry, water depths of ~16 and ~ 22 meters	5e
		Q5c Q5a	112.4 to 77.8	Conch Reef, Looe Key, Carysfort Light area and Molasses Reef	water depth of -15.2 and -15.5 meters (Carysfort Light area)	5c 5a
		Q4b?	230-220	Long Key Quarry	~0.7 to 3.5 meters above sea level	7
		Q4a	340-300	Point Pleasant Core	NR	9
	Fort Thompson Formation	Q3 Q2 Q1 (oldest)	*** *** ***	Grossman Ridge Rock Reef and Joe Ree Rock Reef	NR	11 11 11?

Source: References 928, 929, 930, and 933

Notes:
"?" uncertainty
***** no reliable dates (Reference 928)**
NR- elevations are not recorded in Reference 928
The Radiometric Age Date column is derived from Uranium-series ages ($^{234}U/^{238}U$) on corals and thermal ionization mass-spectrometric Uranium-Thorium (TIMS U-Th) dating.
The Depth Column is approximate.

Figure 2.5.1-355. Locations of the Trail Ridge, Penholoway Terrace and Talbot Terrace in northern Florida and southern Georgia

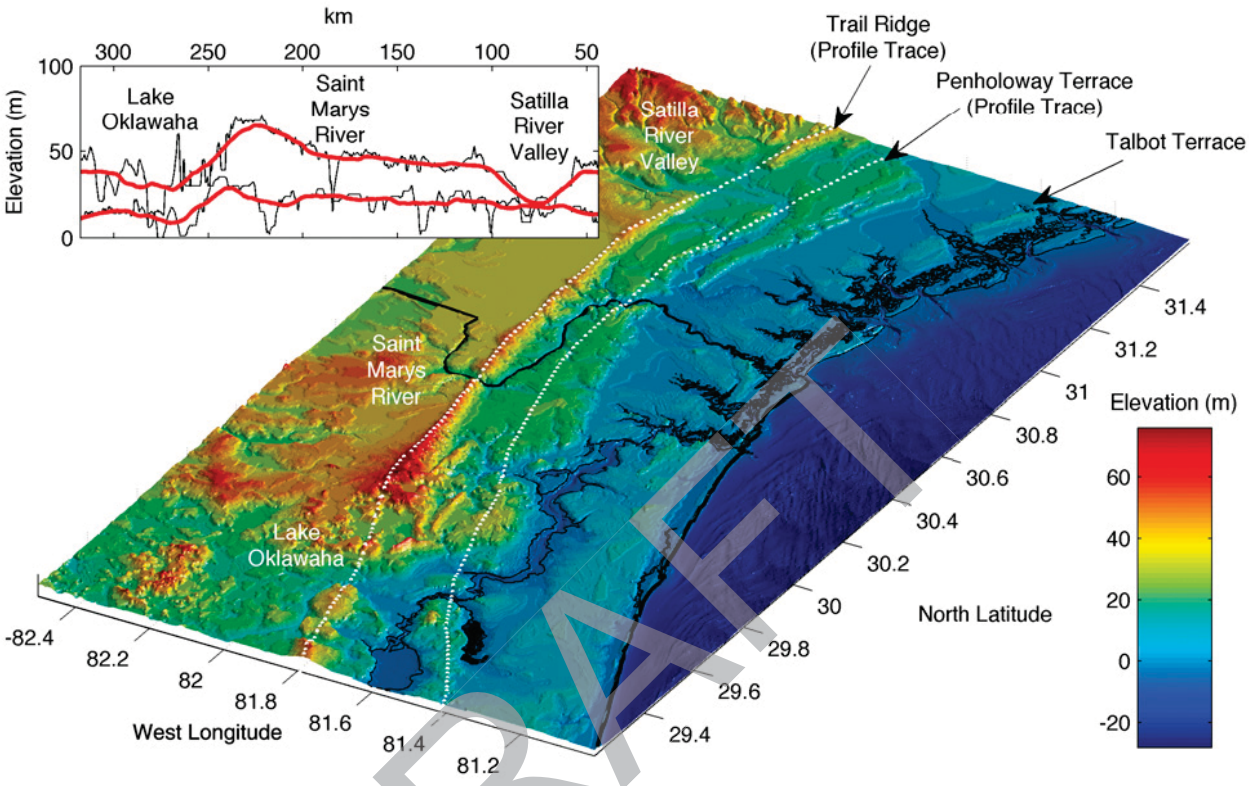

Source: Reference 927

Note: Oblique hill shade image of northern Florida and southern Georgia showing Trail Ridge, modern shoreline, and karstified central Florida. The inset is a profile along Trail Ridge axis showing spatial variation in uplift, which agrees with spatial variation in karstification and/or lithology (Reference 927).

Figure 2.5.1-356. Joe Ree Rock Reef and Grossman Ridge Rock Reef Locations in south Florida in relation to the Turkey Point Units 6 & 7 Site

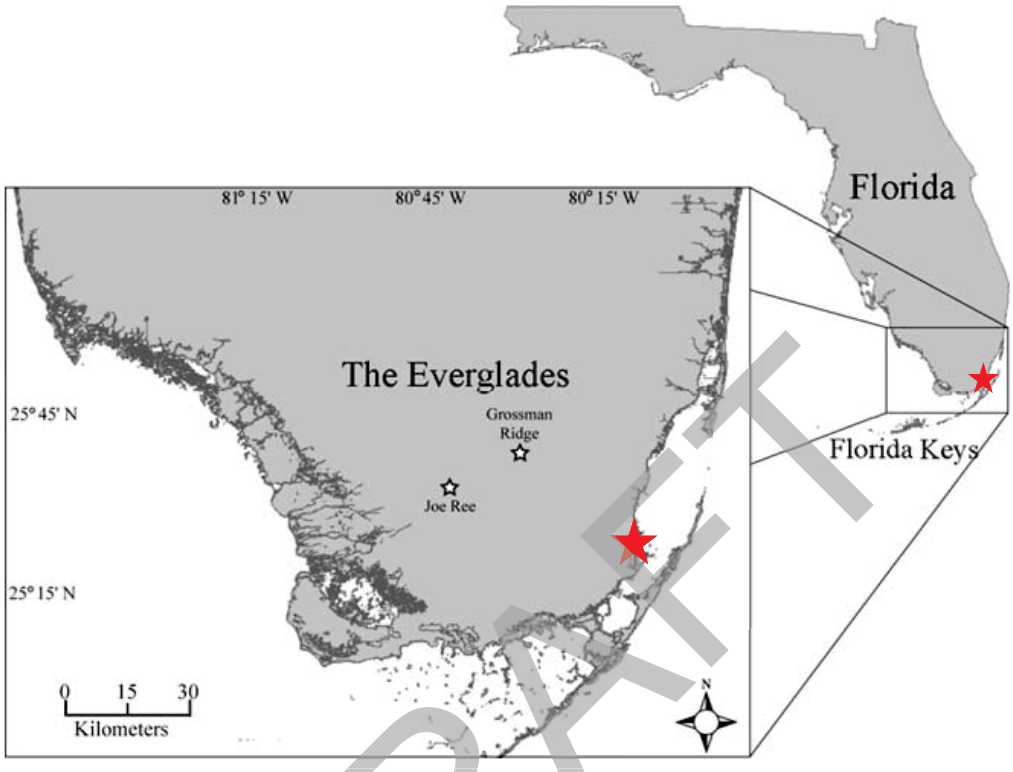

Source: modified from Reference 928

Figure 2.5.1-357. Correlation of marine sequences of the Fort Thompson Formation and Miami Limestone

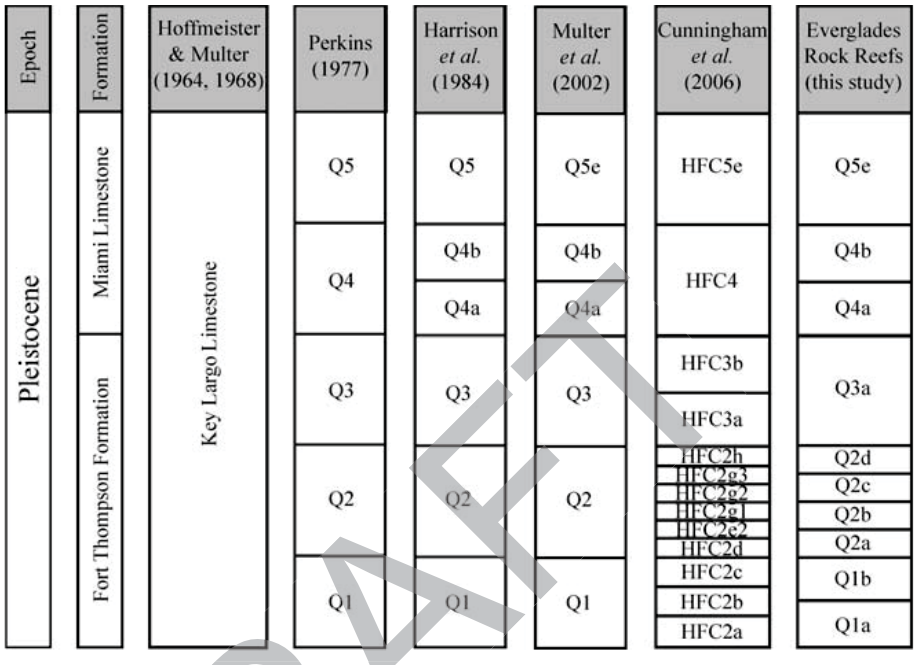

Source: Reference 928

Figure 2.5.1-358. Interpreted correlation of south Florida Pleistocene sea level record

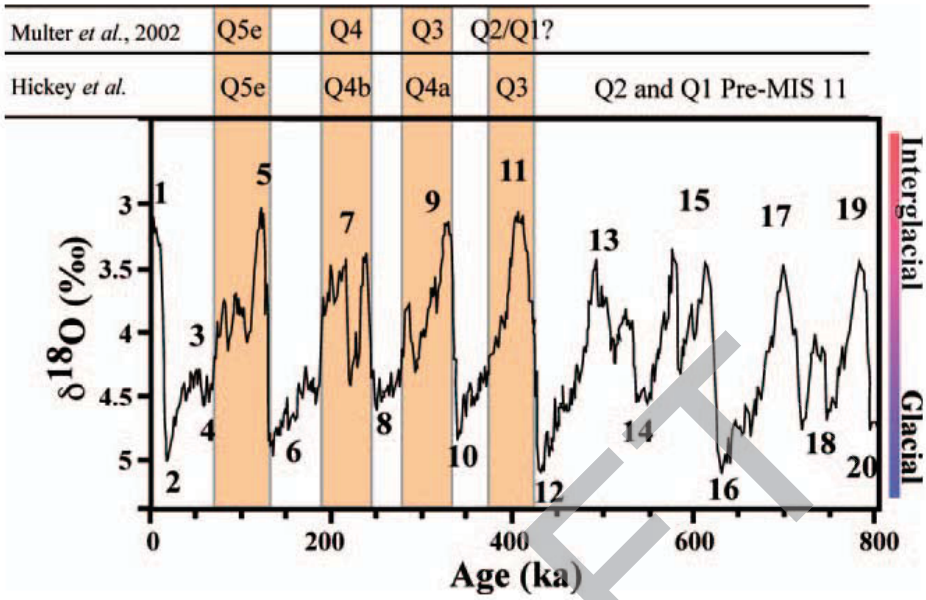

Source: Reference 928

Figure 2.5.1-359. Carysfort Outlier Reef and Sand Key Outlier Reef Locations in south Florida in relations to the Turkey Point Units 6 & 7 Site

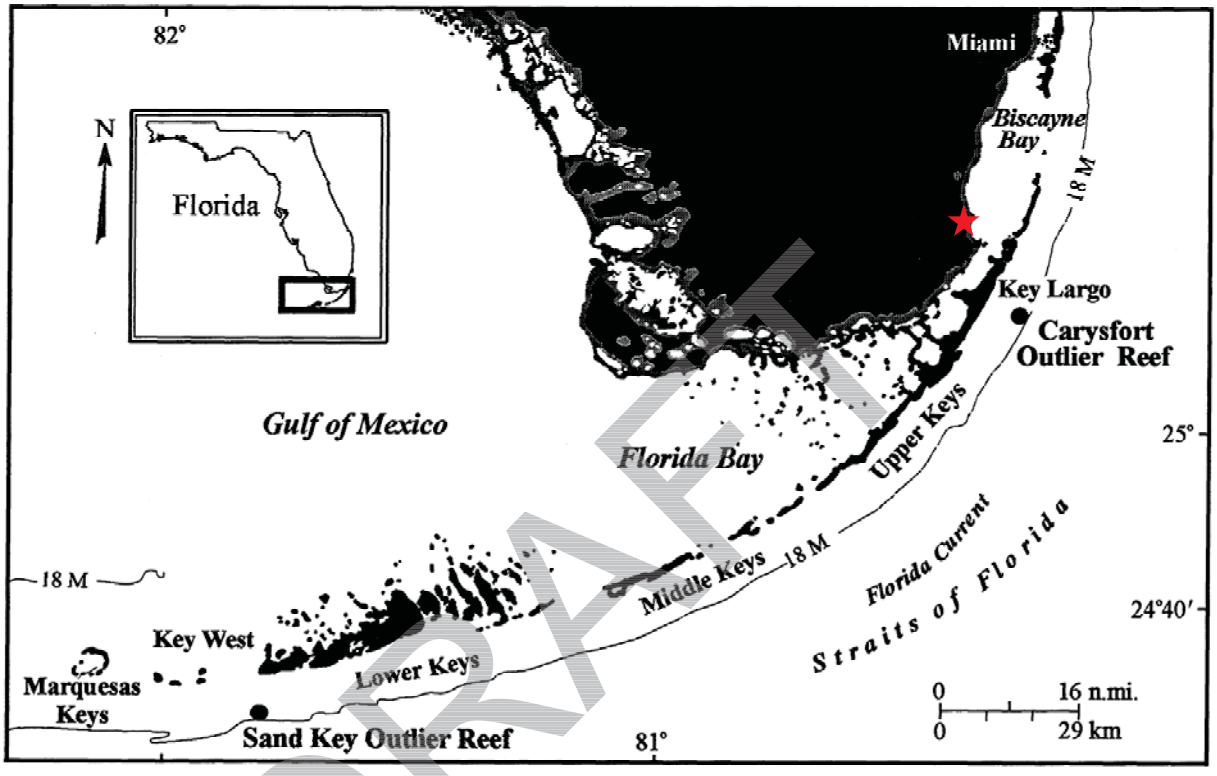

Source: modified from Reference 931

Figure 2.5.1-360 Schematic cross sections of the Sand Key Outlier Reef and the Carysfort Outlier Reef

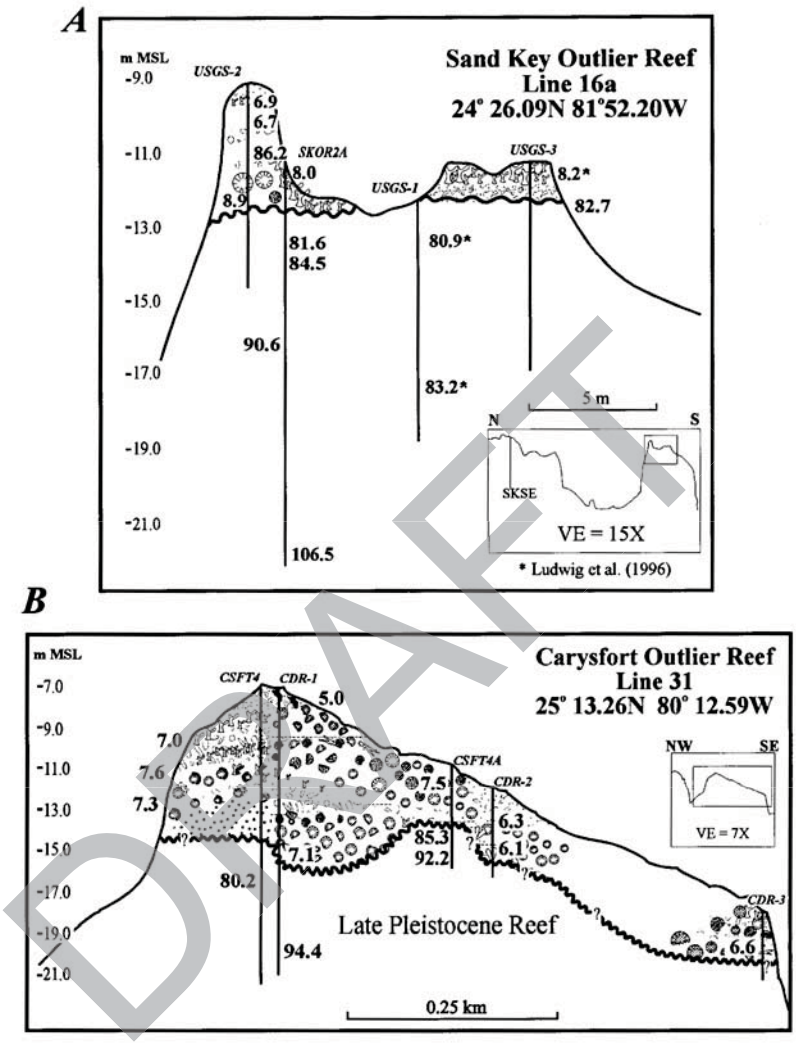

Source: Reference 932

Note: Interpreted cross sections for Sand Key (main outlier reef) and Carysfort Outlier Reef. All dates were determined via the high-precision TIMS U-Th technique. Unconformities were placed using U-Th dates and stable isotope data differentiating marine units from subaerial exposure horizons (Reference 932). All Pleistocene U-Th dates indicate *in situ* post-Substage 5e reef growth. A: Sand Key Cross Section: One Pleistocene date of 86.2 ka in core SKOR2A is considered to be reworked into the associated rubble-pinnacle feature. B: Carysfort Cross Section: All cores are shown. An *A. palmata* reef crest occurs in core CSFT4A (Reference 932).

Figure 2.5.1-361. Composite cross section of the Florida Keys from northwest to southeast and U-series ages of corals from Quaternary reefs.

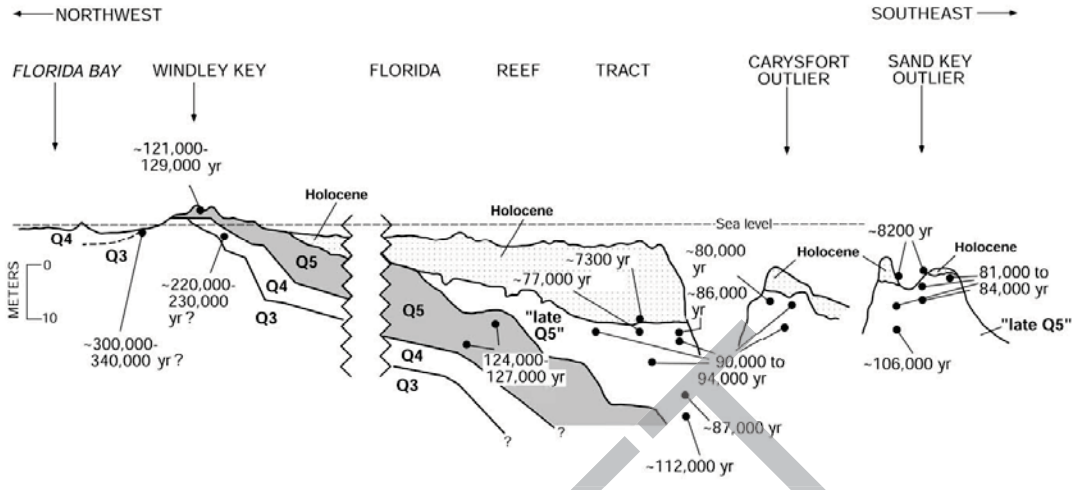

Source: Reference 933

Figure 2.5.1-362 State of Florida showing modern last glacial and last interglacial shorelines and Uranium series age dates of Pleistocene reefs in south Florida in relations to the Turkey Point Units 6 & 7 Site

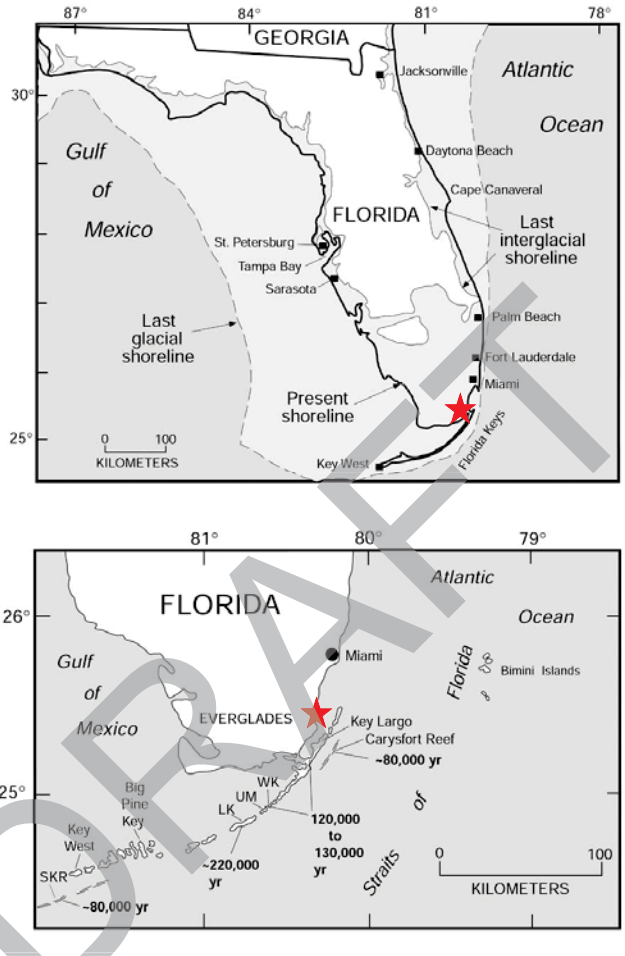

Source: modified from Reference 933

Notes: Upper: map of the State of Florida, showing the modern, last glacial (~21,000 years), and last interglacial (~120,000 years) shorelines. Lower: detail of southern Florida, including the Florida Keys, and U-series ages of emergent or shallow-submerged Pleistocene reefs. Abbreviations: WK, Windley Key, UM, Upper Matecumbe Key; LK, Long Key; SKR, Sand Key Reef (Reference 933).

Table 2.5.1-203 will be updated in a future revision of the FSAR as follows:

Table 2.5.1-203
Regional Marine Terraces, Elevations, and Probable Ages

Terrace Name	Elevation Range (feet above MSL)	Notes	Probable Age[a] [d]
Silver Bluff	1-10	—	0.043 Ma
Princess Anne[c]	10-20	—	0.064 Ma
Pamlico	10-25	—	0.095 – 0.145 Ma
Bethera[b] Talbot [d]	25-42	Formed during pause in sea-level retreat from 100-25 feet	0.210 Ma **0.120** [d]-0.227 Ma
Penholoway[d]	42-70	Formed during pause in sea-level retreat from 100-25 feet	0.393-**0.408** [d] Ma
Wicomico	70-100	Penholoway-Wicomico form single transgressive-regressive sequence	0.393 Ma
Okefenokee[b] Sunderland	100-170	Okefenokee and Sunderland terraces grouped by some authors	0.763 Ma 1.430 Ma
Coharie	170-215	Coharie-Sunderland form single transgressive-regressive sequence	1.650 Ma
Hazelhurst	215-320	—	1.66 to 1.98 Ma(?)

Source: Modified from References 271, 260**, and 927.**

(a) Probable age is a calculated from $\Delta H = kT$ ($k = 0.135 \times 10^{-3}$) with final correlation of high sea level data with deep-sea core stages (Reference 260). Age is given in millions of years before present (Ma).

(b) Based on terrace recognized in southern Georgia; not recognized as a separate terrace in Florida in Reference 271.

(c) The Princess Anne terrace is not seen in Florida but is the ninth terrace that Ward (Reference 260) observes in South Carolina.

(d) The approximate age is derived from modeling precipitation, karstification, isostatic uplift, and sea-level rise (Reference 927).

ASSOCIATED ENCLOSURES:

None

NRC RAI Letter No. PTN-RAI-LTR-041

SRP Section: 02.05.01 - Basic Geologic and Seismic Information

QUESTIONS from Geosciences and Geotechnical Engineering Branch 2 (RGS2)

NRC RAI Number: 02.05.01-6 (eRAI 6024)

FSAR Section 2.5.1.1.1.2.1.1, "Holocene Stratigraphy of the Florida Peninsula" passage states that the general history of sea-level transgression and regression during the Holocene is based on deposits preserved in Blackwater Bay on the southwest Gulf coast of Florida. You state that a significant event, around 1000 to 1090 years before present, is indicated by a sediment layer (Type D) found in all these cores at the same elevation. You suggest that this may be the result of a storm deposit or series of storm deposits. In addition you discuss a model of sea-level transgression, regression, transgression during the Holocene based on Holocene stratigraphy derived from several sources (References 749, 757, 750, 753, 800, 754).

In order for the staff to determine if there is a record of a Holocene tsunami manifested in these deposits and in support of 10 CFR 100.23 please address the following:

a) Discuss the distinction between storm and tsunami deposits. In addition, why are type D sediments not considered a tsunami deposit.
b) Discuss whether the Holocene relative sea level curve in the vicinity of the site correlates or not to the stratigraphic and geographic position of type D sediments and the significant event c.1000 ybp.

FPL RESPONSE:

The RAI refers to "type D" sediments, however, to be consistent with Lowery (FSAR 2.5.1 Reference 750); the deposits are referred to in the response as "Unit D" sediments.

a) Discuss the distinction between storm and tsunami deposits. In addition, why are type D sediments not considered a tsunami deposit.

The distinction between storm and tsunami deposits are discussed in FSAR Subsection 2.5.1.1.5. In summary, the challenge of discriminating between the two types of deposits is that both tsunami and storm surge processes result in the onshore transport and re-deposition of sediments. Tuttle et al. (FSAR 2.5.1 Reference 889) conclude that four discriminators could be used to distinguish between tsunami and storm deposits:

1. Tsunami deposits exhibit sedimentary characteristics consistent with landward transport and deposition of sediment by only a few energetic surges, under turbulent and/or laminar flow conditions, over a period of minutes to hours; whereas, characteristics of storm deposits are consistent with landward transport and deposition of sediment by many more, less energetic surges, under primarily laminar flow conditions, during a period of hours to days.
2. Both tsunami and storm deposits contain mixtures of diatoms indicative of an offshore or bayward source, but tsunami deposits are more likely to contain broken valves and benthic marine diatoms.

3. Biostratigraphic assemblages of sections in which tsunami deposits occur are likely to indicate abrupt and long-lasting changes to the ecosystem coincident with tsunami inundations.
4. Tsunami deposits occur in landscape positions, including landward of tidal ponds, that are not expected for storm deposits.

Similarly, Morton et al. (FSAR 2.5.1 Reference 890) attributes the differences between tsunami and storm deposits to differences in the hydrodynamics and sediment-sorting processes during transport. Morton et al. (FSAR 2.5.1 Reference 890) contends that tsunami deposition results from few high-velocity, long-period waves that entrain sediment from the shore face, beach, and landward erosion zone. Tsunamis can have flow depths greater than 33 feet (10 meters), transport sediment primarily in suspension, and distribute the load over a broad region where sediment falls out of suspension when flow decelerates. In contrast, storm inundation generally is gradual and prolonged, consisting of many waves that erode beaches and dunes with no significant overland return flow until after the main flooding. Storm flow depths are commonly less than 9.8 feet (3 meters), sediment is transported primarily as bed load by traction, and the load is deposited within a zone relatively close to the beach (FSAR 2.5.1 Reference 890). A schematic of typical tsunami and storm deposits is shown in FSAR Figure 2.5.1-348.

Morton et al. (FSAR 2.5.1 Reference 890) report that trench excavations in tsunami deposits often have a mud cap at the surface and rip-up clasts whereas, storm deposits do not. Also, the landward extent of tsunami deposits is generally considered to be greater than that of storm deposits, and tsunami deposits typically occur at higher elevations than storm deposits. These latter criteria are also noted by Tuttle et al. (FSAR 2.5.1 Reference 889).

Based on Shanmugam's (Reference 1) review, the problem of differentiating paleotsunami from paleostorm deposits is not straightforward. The sedimentary records of both types of deposits can exhibit the following sedimentary features: basal erosional surfaces, anomalously coarse sand layers, exotic boulders, imbricated boulders and gravel clusters with imbrications, chaotic bedding, rip-up mud clasts, normal grading, inverse grading, multiple upward-fining units, landward-fining trend, horizontal planar laminae, cross-stratification, richness of marine fossils, changes in chemical elements, and lastly, sand injection and soft-sediment deformation. There are no reliable sedimentological criteria for distinguishing paleotsunami and paleostorm deposits in various environments. Both paleotsunamis (tsunamis) and paleostorms (storms) can generate identical depositional processes and related sedimentary features (Reference 1).

Because of the scouring effect of hurricanes in southern Florida (FSAR References 2.5.1-756, 2.5.1-865, and 2.5.1-866), Holocene sediment sequences are preserved only in protected depositional environments (i.e. in areas that have a dense mangrove forest). The Turkey Point Units 6 & 7 site does not have a dense forest of mangroves; therefore, the environment is not a protected depositional environment, and as a result, physical erosion such as wave action will remove any "paleostorm" deposit(s). Much of the recent work on these paleostorm deposits has focused on low energy, low relief areas sheltered by barrier islands, such as the mangrove-capped oyster bars that separate Florida Bay from open marine influences (FSAR Reference 2.5.1-755). The Unit D sediment facies (changing from

red mangrove peat, Unit C, to a shelly quartz packstone to wackestone, Unit D) is located in Blackwater Bay in southwest Florida and is not present at the Turkey Point Units 6 & 7 site. Based on studies by Tuttle et al (FSAR Reference 2.5.1-899), Morton et al (FSAR Reference 2.5.1-890) and Lowery (FSAR Reference 2.5.1-750), FPL interprets Unit D as a possible storm deposit. The sediment and facies change in the Blackwater Bay example have been interpreted to reflect a storm or a series of storms that dated 1090 +/- 40 years before present (B.P.) (FSAR Reference 2.5.1-750). The radiometric age dates of the sediments correspond to the Medieval Warm Period. Generally, approximately 950 to 1300 years B.P, North America, Europe, and Greenland experienced a warming trend called the Medieval Warm Period (also known as the Medieval Warm Epoch or Medieval Climate Anomaly). During this period, some regions may have experienced higher sea level, high levels of explosive volcanism, warmer temperatures, droughts, exceptional rains (El Niño Southern Oscillation and the Atlantic Multidecadal Oscillation), and greater hurricane frequency (References 2, 3, 4 and 5).

Due to the geomorphic nature of Florida (narrow and low lying and surrounded by the Atlantic Ocean to the east, the Straits of Florida to the south, and the Gulf of Mexico to the west), precipitation is dependent on sea surface temperature. Sea surface temperatures that are 2˚C warmer than present would increase hurricanes four-fold, and 2˚C colder would eliminate them (Reference 5). Warm conditions generally correspond to increased summer rainfall over Florida, and cool conditions correspond to decreased summer rainfall. However, the warm conditions are associated with increased hurricane activity and/or a higher frequency of major hurricanes in the tropical North Atlantic and Caribbean Sea (Reference 4).

Paleoclimate proxies for storms and hurricanes during the Medieval Warm Period are sediment and pollen assemblages. As an example, Cohen et al. (Reference 5) describe a shell ridge on Marco Island that is located behind the low-energy beach with bedding indicating runup and overtopping to a height of 8 feet above present sea level (this is approximately 5 feet higher than the ridges formed in historical time). The shells (*Donax variabilis*) are dated by Carbon-14 methods at 650+/-95 years B.P. and 2,612 +/-59 years B.P. Cohen et al. (Reference 5) postulate that the last contribution to the ridge was during the Medieval Warm Period and that the increased beach ridge height was due to higher sea level and possible hurricanes.

The geotechnical boring logs from the subsurface investigations of the Turkey Point Units 6 & 7 site are described in FSAR Subsections 2.5.1.2, 2.5.4 and in the response to RAI 02.05.01-7. The Holocene sediment (i.e., muck) is sampled in all of the 88 borings. Standard penetration tests (SPTs) and samples of the Holocene sediment are taken at 2.5-foot intervals to a depth of 15 feet. The geotechnical boring logs indicate that geologic conditions are uniform across the site (FSAR Figures 2.5.1-338 through 2.5.1-341 and 2.5.4-203 through 2.5.4-208) and show no depositional evidence of interruption by either a tsunami or storm-like event. Muck is observed in the geotechnical borings and the MASW (Multi-channel analysis of surface waves) data across the site. The muck appears to be thicker in the areas of the surficial dissolution features, which act as sediment traps (FSAR Figures 2.5.4-229 and 230 and the response to RAI 2.5.4-1). The site exploration data do not indicate the presence of erosional channels that are filled with poorly sorted siliciclastics containing exotic fragments or coral rubble that might have been deposited by

paleotsunamis or topographically high areas with potential paleotsunami overwash deposits (FSAR Figure 2.5.1-348).

The conclusion that there are no paleostorm (or paleotsunami) deposits at the site is based on the interpretation of the soil boring data (FSAR 2.5.1 Reference 708). The marl and muck are interpreted to have formed in an anaerobic tidal environment as indicated by the color (i.e., mottled and a wide range of gray to brown coloration), softness, and wetness descriptions (Table 1 in response to RAI 02.05.01-7). The presence of shells and roots is indicative of a calm, low-energy environment of deposition with little to no wave action enabling plants and organisms to grow and thrive. Lastly, the presence of silt in only 1 of the 88 borings and sand in 9 of the 88 borings drilled at the Turkey Point Units 6 & 7 site is not conclusive evidence of either a paleostorm or a tsunami deposit at the site.

b) Discuss whether the Holocene relative sea level curve in the vicinity of the site correlates or not to the stratigraphic and geographic position of type D sediments and the significant event c.1000 ybp.

Units A to D as defined by Lowery (FSAR Reference 750) are located in Blackwater Bay and overlie the Pliocene limestone bedrock. These units were classified as quartz packstone or a clayey quartz sand (Unit A), quartz grainstone (Unit B), Rhizophora, red mangrove peat (Unit C), and shelly quartz packstone to wackestone (Unit D). Each unit represents a time-transgressive unit as changes in sea level caused migration of the depositional environments. Units A and B formed during the early transgressive phase as shoreline approached landward. Unit C represents the relative shallowing or temporary stabilization of the shoreline or an intertidal regime and Unit D represents a reinitiation of a relative sea-level rise and a return to deeper water conditions (FSAR 2.5.1 Reference 750).

The Unit D sediment surface contains indications of increasing water depths followed by shallower water depths as seen by the overlying oyster beds on the finer muds of the deeper depositional environment. The oyster beds are indicative of an intertidal environment. Previous cores show a sequence of mangrove-capped oyster bars over these finer muds. During the initial flooding of the mangrove system, the “waterflow and sedimentation process may not have been ideal for oyster habitation, but a slight increase in depth may have allowed initiation of oyster colonization and sediment aggradation” (FSAR 2.5.1 Reference 750).

Furthermore, an upstream carbonate mud levee in the Blackwater River contains marine faunal fragments 1069 +/- 99 years B.P. to 990 +/-84 years B.P. in age (Figure 1). A possible interpretation of this levee is that it is the result of landward transport and deposition of marine sediment and fauna during a violent storm event or a period of high storm frequency. These age dates correspond to the dates of the submergence of mangroves in Blackwater Bay (Figure 1, Transgression 2) (FSAR 2.5.1 Reference 750). The Holocene sea-level curve in the vicinity of the site correlates to the stratigraphic and geographic position of Unit D sediments and their corresponding significant event approximately 1000 to 1090 years B.P (Figure 1, green star).

Figure 1 Holocene Sea Level Rise Curve Illustrating Deceleration of Rate of Rise and Present Rapid Rise from Tide-Gauge Records (modified from FSAR 2.5.1 Reference 750)

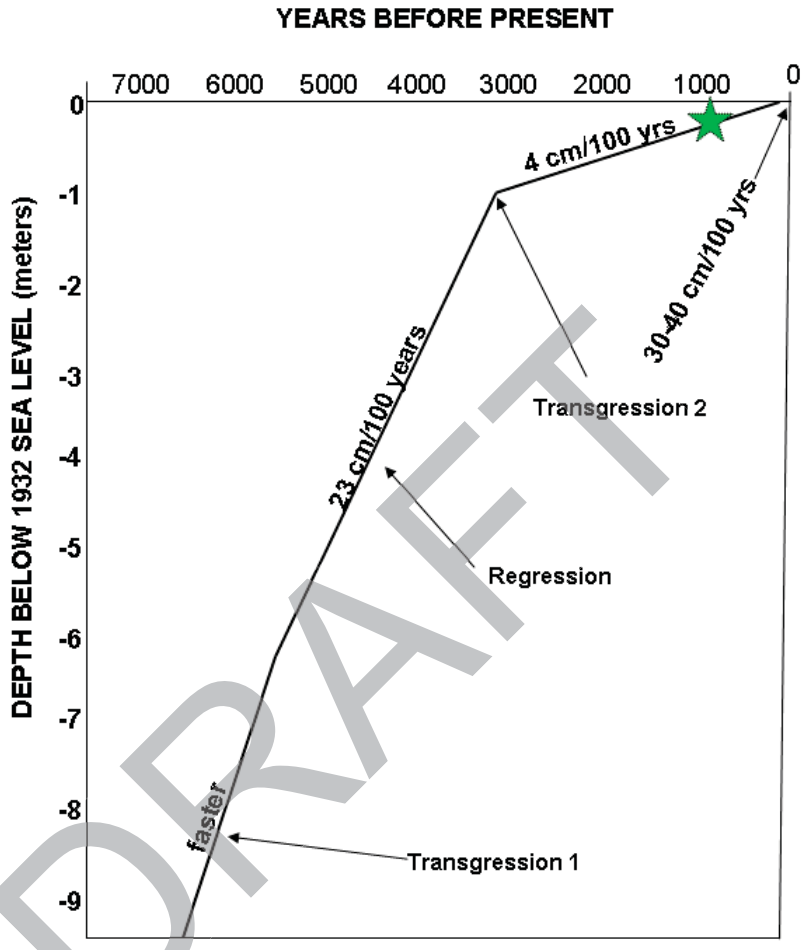

Note: The green star denotes the stratigraphic and geographic position of Unit D sediments and their corresponding significant event ~ 1000 to 1090 years B.P.

This response is PLANT SPECIFIC.

References:

1. Shanmugam, G., "Process-sedimentological challenges in distinguishing paleo-tsunami deposits," *Natural Hazards*, Springer, 2011.
2. Xoplaki, E., Fleitmann, D., and Diaz, H., Editorial: "Medieval Climate Anomaly," in *PAGES news: Medieval Climate Anomaly*, Xoplaki, E., Fleitmann, D., Diaz, H., von Gunten, L., and Kiefer, T. (eds.), Vol. 19, No. 1, pp.4, 2011.
3. Bradley, R., Hughes, M., and Diaz, H., "Climate in Medieval Time," *Science*, Vol. 302, pp. 404–405, 2003.
4. Albritton, J., *A 1700-Year History of Fire and Vegetation in Pine Rocklands of National Key Deer Refuge, Big Pine Key, Florida: Charcoal and Pollen Evidence from Key Deer Pond*, Master's Thesis, University of Tennessee, 2009.
5. Cohen, A., Gleason, P., Brooks, H., Stone, P., Goodrick, R., Smith, W., and Spackman, W., *The Environmental Significance of Holocene Sediments from the Everglades and Saline Tidal Plain, in Environments of South Florida Present and Past II*, Gleason, P. (ed.), Miami Geological Society, Coral Gables, Florida, pp. 297–351, 1984.

ASSOCIATED COLA REVISIONS:

None

ASSOCIATED ENCLOSURES:

None